P148588.PDF [Page: 3 of 88]

93-654

COMMUNICATIONS
RESEARCH
LABORATORY

A Study of Track Initiation and Data Association for Multiple Target Tracking

Ji Chen
Titus Lo
John Litva

This report applies to DSS contract No. W7714-2-9619-101-ST
June, 28th, 1993

Faculty of Engineering
McMaster University
Hamilton, Ontario
Canada L8S 4K1

CRL Report No. 271

P148588.PDF [Page: 4 of 88]

Contents

1 Introduction 6

2 Track Initiation 9

3 Gating 20

4 Filtering and Prediction 24

5 Data Association 30

6 Direction weighting data Association 37

7 Neural Network for Data Association 49

7.1 Traveling Salesman Problem (TSP) 49

7.2 Hopfield Neural Network for the Data Association in Multiple Target Tracking 50

7.3 Boltzmann machine and simulated annealing for data association 55

8 Real Data and Simulation Test 63

P148588.PDF [Page: 5 of 88]

105-02510/

9 Conclusions and Recommendations **77**

P148588.PDF [Page: 6 of 88]

List of Figures

2.1 Normal parametric representation of a straight line 10

2.2 Histogram in $\rho - \theta$ space 12

2.3 $\rho - \theta$ relation 13

2.4 Tolerance range must be set for the initiation 14

2.5 Illustration of the angle criterion in our initiation 16

2.6 Comparison of probability of detection between our proposed initiation algorithm and standard Hough Transform initiation algorithm. — New initiation algorithm. - - Standard Hough transform initiation 18

2.7 Comparison of false alarm rate between our proposed initiation algorithm and standard Hough Transform initiation algorithm. — Standard Hough Transform initiation algorithm - - New initiation algorithm 19

4.1 Flow diagram of filtering and prediction 25

P148588.PDF [Page: 7 of 88]

5.1 Illustration of data association 32

6.1 Condition to generate apparent motion perception 38

6.2 Perception based association during apparent motion 40

6.3 Generation pseudo direction 41

6.4 Percentage of track loss in clutter environment. — PDA - - DPDA -.- NN 45

6.5 Percentage of track loss in different noise environment — Nearest Neighbor - - PDA -. DPDA 46

6.6 Tracking real data using standard nearest neighbor algorithm . . . 46

6.7 Tracking real data using Probability Data Association algorithm . . 47

6.8 Tracking real data using Direction weighting Probability Data Association algorithm 47

7.1 Typical problem of TSP 51

7.2 Array of interconnected neurons with input currents and output voltage 51

7.3 A typical output of Hopfield neural network 54

7.4 A valid Boltzmann machine configuration for computing the JPDA data association probabilities 58

8.1 Two kinds of tracks that should be deleted 65

8.2 Measured data of R1T1. 67

P148588.PDF [Page: 6 of 88]

8.3 Tracking R1T1 data using direction probability data association . . 68
8.4 Tracking R1T1 data using Hopfield neural network to implement JPDA 69
8.5 Measured data of R1T2 69
8.6 Tracking result of R1T2 using direction PDA 70
8.7 Tracking R1T2 data using Hopfield neural network to implement JPDA 70
8.8 Measured data of R2T1 71
8.9 Tracking result of R2T1 using direction PDA 71
8.10 Measured data of R2T2 72
8.11 Tracking result of R2T2 using direction PDA 72
8.12 Measured Lab data 73
8.13 Tracking Result of Lab data using Nearest Neighbor data association 73
8.14 Tracking Result of Lab data using Probability data association . . . 74
8.15 Tracking Result of Lab data using direction probability data association 74
8.16 Simulation result of Boltzmann machine implemented JPDA when the number of target is two 75
8.17 Simulation result of Boltzmann machine implemented JPDA when the number of target is four 75
8.18 Tracking real data using Boltzmann machine to implement JPDA . 76

Chapter 1

Introduction

The problem of tracking simultaneously many moving targets in clutter environments has received much renewed attention in recent years because of its potential application in the strategic defense system. It also finds applications in the fields of air traffic control and security surveillance system. The objective of multiple target tracking is to partition the sensor data into sets of observation, or tracks, produced by the same source. Once tracks are formed and confirmed (so that background and other false targets are reduced), the number of targets can be estimated and quantities, such as target velocity, future predicted position can be computed for each track.

The basic process of MTT (Multiple Target Tracking) can be divided into three stages. They are track initiation (birth), track maintenance (life), and track deletion (death). In a real system, these three stages should be simultaneously carried out since new tracks may appear, while old tracks may be losted at any time. A good multiple-target tracking system

P148588.PDF [Page: 10 of 88]

should be able to establish new tracks and delete the lost tracks.

With the advent of Kalman filtering technique in early 1970's, the recursive target state estimation becomes available. Kalman filter minimizes the mean–square error as long as the target dynamics and measurement noise are well modeled. The adaptive gain in Kalman filter can provide high accuracy in estimation.

The essential part in the MTT system is data association and extensive work has been carried out in this area. It is the process of assigning measurements to existing tracks. The mostly used algorithms for MTT are Nearest Neighbor (including general N. N.)Data Association, Tracking–Splitting Data Association, Probability Data Association and Joint Probability Data Association. Each algorithm has its own advantages and disadvantages. It is the trade–off between estimation accuracy and computational complexity. In this report, nearest neighbor, PDA and JPDA with neural implementation are investigated.

It is known that the target's next possible location is also closely related to its heading which is associated with the target's speed direction. Thus, based on the idea of motion perception, directional weighting is incorporated into the probability calculation of PDA, which improves the performance of the PDA algorithm.

Neural networks are new emerging technologies in recent years and has been introduced into data association for MTT. Two kinds of neural networks (Hopfield neural network and Boltzmann machine) are investigated and evaluated in report.

This report consists of nine chapters. In Chapter 2 detailed procedures of our new track initiation algorithm. are described. In Chapter 3 is presented the Gating technique in

P148588.PDF [Page: 11 of 88]

MTT. In Chapter 4, we review the concept of Kalman filter in MTT problem and how it is implemented in our system. In Chapter 5 data association in the MTT system is discussed and PDA is described in details. The nearest–neighbor data association is compared with proability data association based on simulations as well as the real data. Motion perception based direction weighting is used in Chapter 6 to improve the efficiency of tracking and in Chapter 7 two kinds of neural networks are investigated for MTT problem. In Chapter 8, more real data are used to test the algorithms and in Chapter 9 are given the conclusions and recommendations.

Chapter 2

Track Initiation

A number of tracking algorithms have been developed and they can be found in the open literatures. However, in most of these algorithms, it is assumed that the existence of tracks and the number of tracks are known. In the PDA tracker, computational load does not increase rapidly with increasing numbers of targets, but unfortunately it suffers from the inability to initiate tracks on new targets by itself. For this reason, a separate track initiation algorithm is required to identify tracks from high density clutter environment. Only after we obtained the confirmed the tracks can we begin to estimate the targets position and implement the whole tracking algorithms. In this chapter, a new tracking initiation algorithm as well as the standard Hough transform initiation is discussed.

Hough transform is one of the most referred approaches that is used to identify straight lines from clutter environments. This method is based on the fact that, as illustrate in

P148588.PDF [Page: 13 of 88]

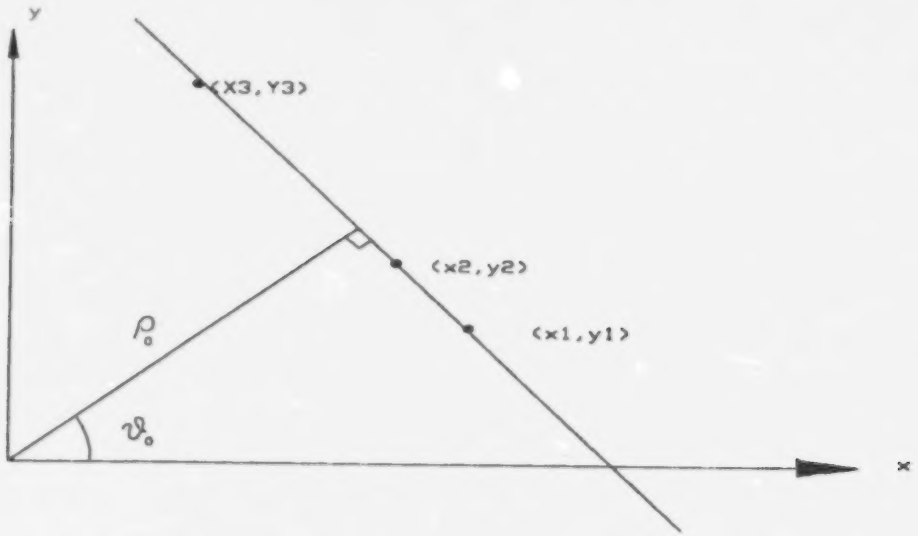

Figure 2.1: Normal parametric representation of a straight line

Fig. 2.1, all points (x_i, y_i) along a straight line have the relation,

$$x_i \cos\theta_0 + y_i \sin\theta_0 = \rho_0 \tag{2.1}$$

where θ_0 is a certain angle with the X axis and ρ_0 is the perpendicular distance of the line from the origin. Thus, all points (x_i, y_i) along the line will have a common (ρ_0, θ_0) in the $\rho - \theta$ parameter space.

In image processing, it is well known that a point (x_i, y_i) in the X–Y plane can be mapped into a curve in the $\rho - \theta$ plane defined by the general relationship (Hough Transform),

$$\rho = x \cos\theta + y \sin\theta \tag{2.2}$$

with θ ranging from 0° to 180°. Since each point in the X–Y plane defines a curve in the $\rho - \theta$ plane, a family of curves can be generated in the $\rho - \theta$ plane based on points in the

P148588.PDF [Page: 14 of 88]

X–Y plane. The family of curves corresponding to points on a straight line will intersect at the (ρ_0, θ_0). Thus, a group of points on the X–Y plane that have the common intercept (ρ_0, θ_0) on the $\rho - \theta$ plane can be identified as a straight line. This may help us to determine the straight–line target trajectories against a heavy clutter background.

For a set of observations, if the total number of increments in the θ paramenter is $N_\theta = \frac{\pi}{\Delta}$, then the center points of the histogram bins will be

$$\theta_1 = \frac{\Delta\theta}{2}, \theta_2 = \frac{3\Delta\theta}{2}, \cdots \theta_{N_\theta} = (N_\theta - \frac{1}{2})\Delta\theta, \tag{2.3}$$

which defines a set values of ρ correspond to θ. Each point contributes to the histogram values for N_θ bins. For random points the contribution will be spread over the bins. On the other hand, points on a straight line will contribute mostly to a particular pin or its adjacent bins. If the number of points within a certain bin exceeds the threshold, a track is declared. In Fig. 2.2, a typical histogram in the $\rho - \theta$ space is shown. From the figure, we can see that there is a possible track located along the line determined by $\rho_0 = 3$ and $\theta_0 = 110°$ in X–Y space.

Hough transform initiation is quite efficient when it is used to detect straight lines in large number of observations. A track is determined by detecting the peaks in the $\rho - \theta$ space. However it does have limitations in a real system. First, in a clutter environment where clutters may form false lines, Hough transform initiation is not able to distinguish them from real lines and declares them as tracks. Second, to detect a peak in $\rho - \theta$ space, a threshold must be used for distinguishing the peaks associated with real tracks form the peaks

P148588.PDF [Page: 15 of 88]

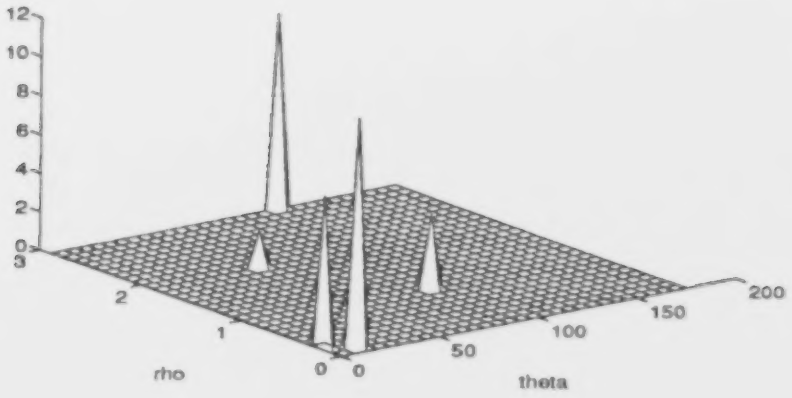

Figure 2.2: **Histogram in $\rho - \theta$ space**

due to clutters. It requires a relatively large number of scans to establish peaks in $\rho - \theta$ space and the threshold for detecting the peaks is difficult to determine. Furthermore, in a real system where a target track must be identified in few scans, the standard Hough transform initiation can yield false detection of target tracks. A modified Hough transform initiation is therefore developed to overcome these difficulties. This modified Hough transform initiation combines the idea of Multiple Hypothesis Tracking (MHT) with the Hough transform. Only few scans data are required.

Like the standard Hough transform, the first step is to locate lines in a composite image containing the superposition of candidate target detections in a series of scans. The targets we considered have curve trajectories which can be approximate as straight line over reasonably short time interval. Following Eq. 2.2, the Hough transform maps several points into

P148588.PDF [Page: 16 of 88]

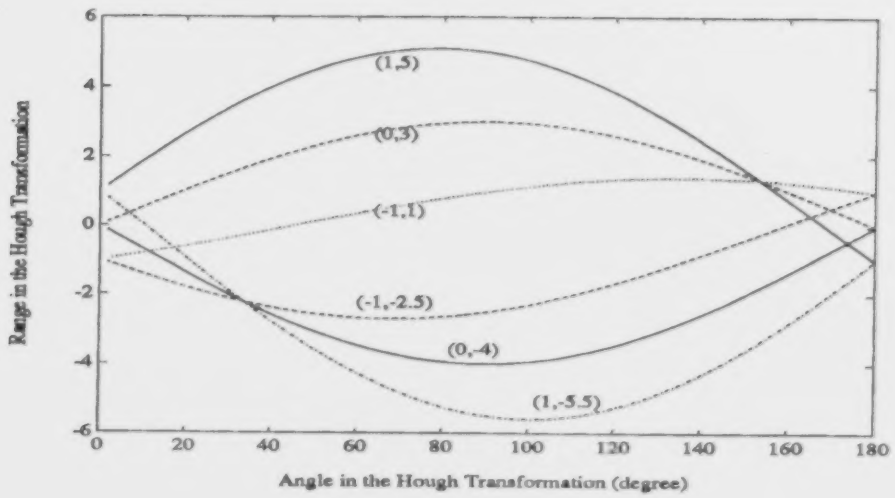

Figure 2.3: $\rho - \theta$ relation

curves in $\rho - \theta$ space as shown by Fig. 2.3. The curves in the $\rho - \theta$ space that correspond to colinear points which form a straight lines will intersect each other at the same point.

Suppose we receive three reports r_n, r_{n+1}, and r_{n+2} at scans $n, n+1$, and $n+2$. Based on these three data points, we obtain three curves ρ_n, ρ_{n+1}, and ρ_{n+2} in the parameter space. The difference function is formed as

$$\Delta\rho_n = \rho_n - \rho_{n+1} \tag{2.4}$$

There are two pieces of information that can be derived from the zero crossing of $\Delta\rho_n$, denoted by $\Delta\rho_n(0)$. First, it indicates the coordinate in θ of the intercept point of ρ_n and ρ_{n+1}, which is denoted by $\theta_{\Delta\rho_n(0)}$. Second, if we consider the points in the image space as vectors, the sign of the slope at the zero crossing depends on the pointing direction of the vector $(\mathbf{r}_n - \mathbf{r}_{n+1})$. Based on these two pieces of information, two criteria are established for

P148588.PDF [Page: 17 of 88]

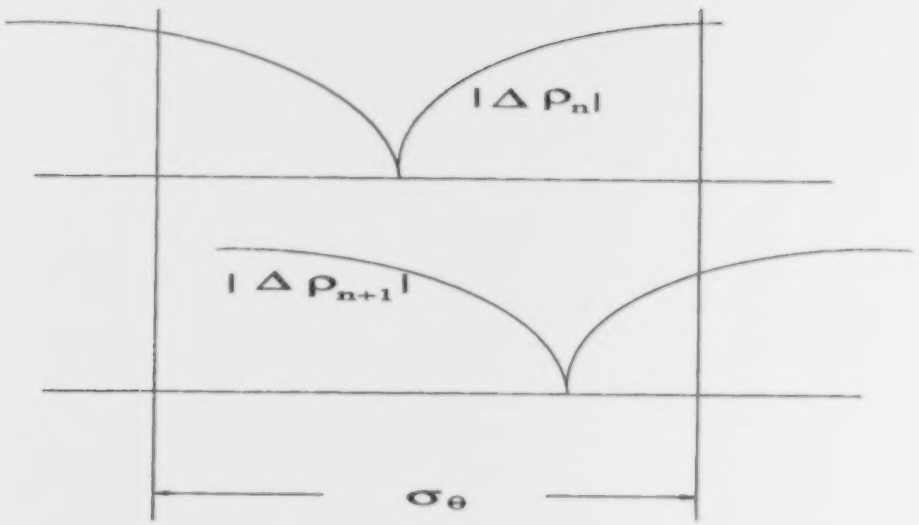

Figure 2.4: Tolerance range must be set for the initiation

track initiation:

1. The zero crossing points $\theta_{\Delta\rho_n(0)}$ and $\theta_{\Delta\rho_{n+1}(0)}$ must be at the same proximity; i.e.

$$| \theta_{\Delta\rho_n(0)} - \theta_{\Delta\rho_{n+1}(0)} | \leq \sigma_\theta, \tag{2.5}$$

   where $\Delta\theta \leq \sigma_\theta \leq m\Delta\theta$ is a tolerance value, as shown in Fig. 2.4, and m is any positive integer.

2. The slopes at the zero crossing points $\theta_{\Delta\rho_n(0)}$ and $\theta_{\Delta\rho_{n+1}(0)}$ must be the same sign.

If both the criteria are satisfied, we say that r_n, r_{n+1}, and r_{n+2} are colinear and they form a possible track. Using criteria (1) and (2), we further test three points r_{n+2}, r_{n+3} and r_{n+4} from scan $n+2$, $n+3$ and $n+4$ to see if they are colinear and can form a possible track.

If points r_n, r_{n+1} and r_{n+2} form a possible track and points r_{n+2}, r_{n+3} and r_{n+4} also form

P148588.PDF [Page: 18 of 88]

a possible track, then we connect these two possible tracks together and recorded these five points as assumed track. This assumed track will be tested further.

By denoting distance between point r_{n+1} and point r_{n+2} as $d_{n+1,n+2}$ and defining the acute angle between vectors $(\mathbf{r}_{n+1} - \mathbf{r}_{n+2})$ and $(\mathbf{r}_{n+2} - \mathbf{r}_{n+3})$ as α_{n+2}, two criteria are developed to test the assumed tracks

1. The acceleration of a target is physically limited, i.e.

$$| d_{n+1,n+2} | \leq 10 \times d_{n+2,n+3} \tag{2.6}$$

2. If five points are approximately on a straight line as shown in Fig. 2.5, we should have

$$\beta_1 \leq \alpha_{n+2} \leq \beta_2 \tag{2.7}$$

where β_1 and β_2 are limiting angles, which have the value to prevent V shape initiated tracks.

If these two criteria are satisfied by the assumed track, we then say points r_n, r_{n+1}, r_{n+2}, r_{n+3} and r_{n+4} form a track. This initiator is implemented in our MTT system at every scan.

Simulations were carried to study the performance of the initiator. In Fig. 2.6 is shown the comparison of of probability of detection, at different noise level, for standard Hough transform initiation and the modified Hough transform initiation. The proability of detection is defined as

$$p_d = \frac{N_d}{N_t} \tag{2.8}$$

P148588.PDF [Page: 19 of 88]

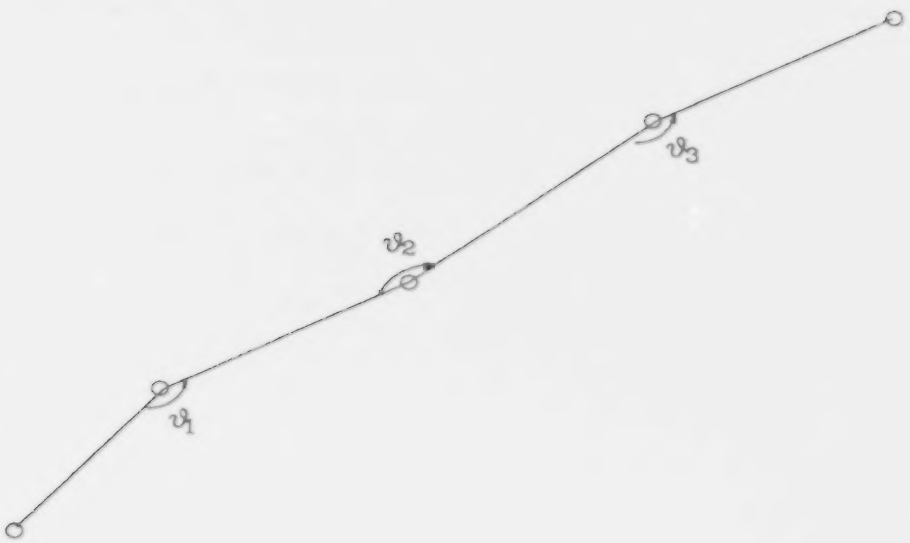

Figure 2.5: **Illustration of the angle criterion in our initiation**

where N_d = total number of detected tracks,

N_t = total number of tracks.

and the noise is a normally distributed. Each curve in Fig. 2.6 is obtained by using 1000 trails. We can see that two kinds of initiation algorithm have very close performance in terms of probability of detection under a noisy environment.

In Fig. 2.7 is shown the comparison of the false track rates, at different levels of clutter-to-target ratio $r_{c/t}$, for both the standard Hough transform initiation and the modified Hough transform initiation. The false track rate is defined as

$$p_f = \frac{N_f}{N_t} \tag{2.9}$$

P148588.PDF [Page: 20 of 88]

where $\overline{M}_c$ = mean number of clutters in a single scan,

M_t = number of true targets in a single scan.

The clutter-to-target ratio is defined as

$$r_{c/t} = \frac{\overline{M}_c}{M_t} \tag{2.10}$$

where $\overline{M}_c$ = mean number of clutters in a single scan,

M_t = number of true targets in a single scan.

The actual number of clutters M_c is a random process, which is assumed to be Poisson distributed. The distribution of the clutter locations in the image space is assumed to be uniform. Each value of p_f in the figure is obtained using 1000 trials. It can be seen that the false track rate is reduced greatly by using the modified HT for track initiation.

P148588.PDF [Page: 21 of 88]

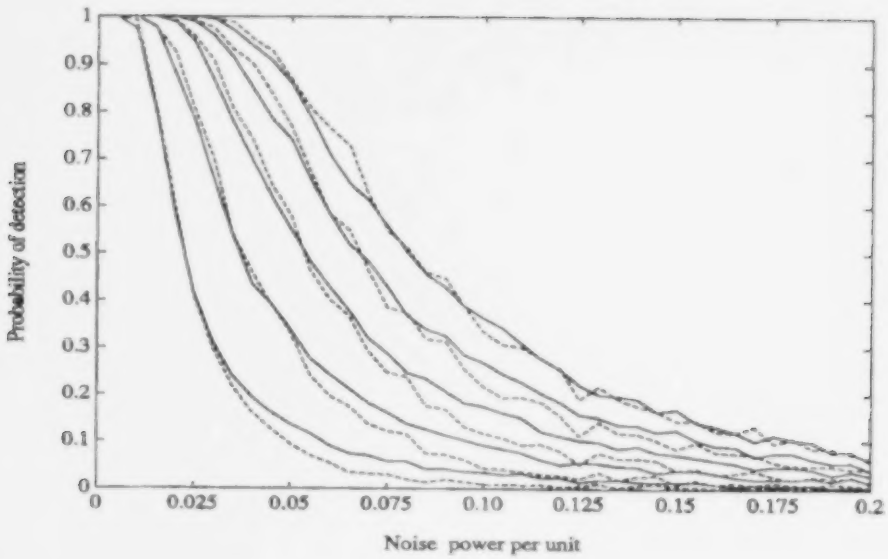

Figure 2.6: **Comparison of probability of detection between our proposed initiation algorithm and standard Hough Transform initiation algorithm. — New initiation algorithm. - - Standard Hough transform initiation**

P148588.PDF [Page: 22 of 88]

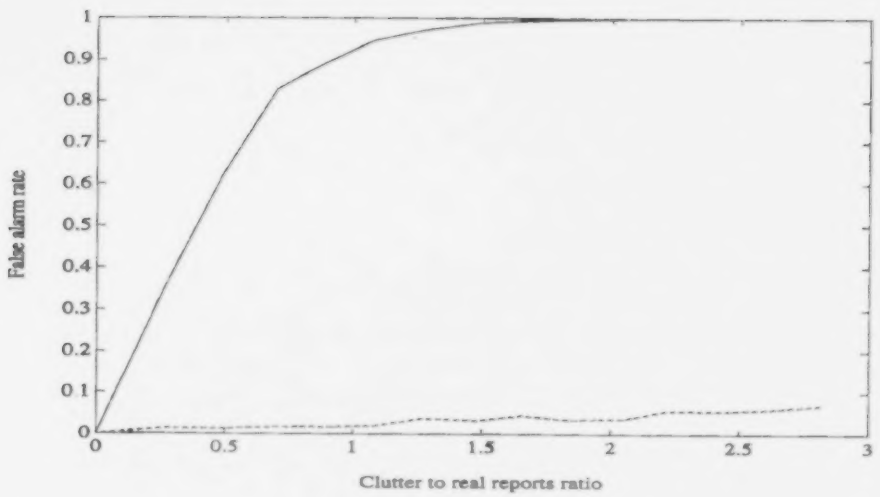

Figure 2.7: **Comparison of false alarm rate between our proposed initiation algorithm and standard Hough Transform initiation algorithm.** — **Standard Hough Transform initiation algorithm** - - **New initiation algorithm**

Chapter 3

Gating

Following the procedure of track initiation, confirmed tracks are selected from the observations. These tracks must be updated as more observations are available. When a set of observations is received, it may be used to update the existing tracks or to initiate new tracks. Because not all the observations can be associated with the existing tracks. The gating technique is needed to eliminate the unlikely observation–to–track parings. Gates are formed around the predicted track position. If a single observation is within a gate and outside the gates of any other tracks, this observation is used to update the track. If more than one observation are found within a gate or the observation is within the gates of more than one track, further logic is required to associate it with tracks. This will be discussed in a later chapter.

In multiple target tracking, it is well known that a measurement at scan k is given by:

$$z(k) = Hx(k) + v(k) \tag{3.1}$$

P148588.PDF [Page: 24 of 88]

where H is the measurement matrix and $v(k)$ is the zero-mean white Gaussian noise with covariance R_c. x is the state vector that includes the quantities to be estimated. The predicted value of scan k is by $\hat{x}(k \mid k-1)$, so the vector difference between the measured and predicted is

$$\tilde{y}(k) = z(k) - H\hat{x}(k \mid k-1) \tag{3.2}$$

$\tilde{y}(k)$ is defined as the residual vector and the residual covariance matrix is, $S = HPH^T + R_c$, where P is the one-step prediction covariance matrix.

Defining d^2 to be the norm of the residual vector, $d^2 = \tilde{y}^T S^{-1} \tilde{y}$, the M-dimensional Gaussian probability density for the residual is

$$f(\hat{y}) = \frac{e^{-\frac{d^2}{2}}}{(2\pi)^{\frac{M}{2}}\sqrt{\mid S \mid}} \tag{3.3}$$

where $\mid S \mid \triangleq$ the determinant of S.

It is clear that with infinite gate size, the correlation performance is optimal. However, the primary purpose of gating logic is to reduce the number of observation-to-track pairing that must be considered, a finite gate size would be appreciated even in those case.

Define a gate (G) such that the measurement will be considered if the following relationship is satisfied by the norm (d^2) of the residual vector:

$$d^2 = \tilde{y}^T S^{-1} \tilde{y} \leq G \tag{3.4}$$

A maximum likelihood gate (G_0) can be defined such that an observation falling within that gate is more likely from the track. This gate is defined in terms of the probability of detection (P_D), the new source density (β), the measurement dimension (M), and the

P148583.PDF [Page: 25 of 88]

residual statistics as presented by the determinant of the residual covariance matrix ($\mid S \mid$)

$$G_0 = 2ln\frac{P_D}{(1-P_D)\beta(2\pi)^{\frac{M}{2}}\sqrt{\mid S \mid}} \tag{3.5}$$

The simpler, but less adaptive, method is to choose G based on the chi-square (X^2_M) distribution with M degrees of freedom. Using the chi-square distribution and assuming an allowable probability ($\bar{P_G} = 1 - P_G$) of a valid observation falling outside the gate, the value of G can be determined using a chi-square table and the relationship

$$P_r\{d^2_M > G\} = \hat{P_G} \tag{3.6}$$

The probability (P_G) that a valid observation will fall within the gate G can be formed using the chi-square table. Alternatively, defining a constant likelihood ellipsoid, we have

$$P_G = \int \cdots \int f(\tilde{y})d\tilde{y_1} \cdot d\tilde{y_M} \qquad \text{over ellipsoidal volume} \tag{3.7}$$

For the two dimension case, $P_G(2) = 1 - exp(\frac{-G}{2})$. We select the correct return fallen within the gate with probability of 99%, so the normalized gate size is 9.2. This gate size is chosen in our system.

Once the gate has been formed, all the new observations within the gate will be assigned a likelihood function. Assume the Gaussian distribution for the residual, the likelihood function of observation j associated with track i is:

$$g_{ij} = \frac{e^{-\frac{d_{ij}{}^2}{2}}}{(2\pi)^{\frac{M}{2}}\sqrt{\mid S_i \mid}} \tag{3.8}$$

where S_i is the residual covariance matrix for track i,

$$d^2_{ij} = \tilde{y}^T_{ij}S^{-1}\tilde{y}_{ij} \tag{3.9}$$

P148588.PDF [Page: 26 of 88]

$\tilde{y}_{ij}$ = residual vector from observation j to track i

This likelihood function is a key parameter in MTT and will be used later in the data association algorithm. Another point we should mention is that the new observations are not directly used in the likelihood function, the Kalman filtered result is used in the likelihood function.

P148588.PDF [Page: 27 of 88]

Chapter 4

Filtering and Prediction

In multiple target tracking, filtering and prediction are the techniques that estimate target's present and future kinematic quantities such as position, velocity, and acceleration. Two kinds of filtering technique have been proposed for multiple target tracking. One approach uses fixed tracking coefficients, such as $\alpha - \beta$ and $\alpha - \beta - \gamma$ filter. The other approach generates time–variable tracking coefficients that are determined by a *priori* models for the statistics of measurement noise and target dynamics, it is called Kalman filtering. The first approach has computational advantages for systems with large numbers of targets. However, with expanding computer capabilities, the high–accuracy tracking associated with Kalman filtering is becoming increasingly more appealing to the multiple target tracking designer.

Fig. 4.1 gives a flow diagram of Kalman filtering. The target is characterized by a state vector x which will include quantities such as position, velocity and acceleration. The observation (Z) is assumed to be linear combination of the states (Hx) corrupted by additive

P148588.PDF [Page: 28 of 88]

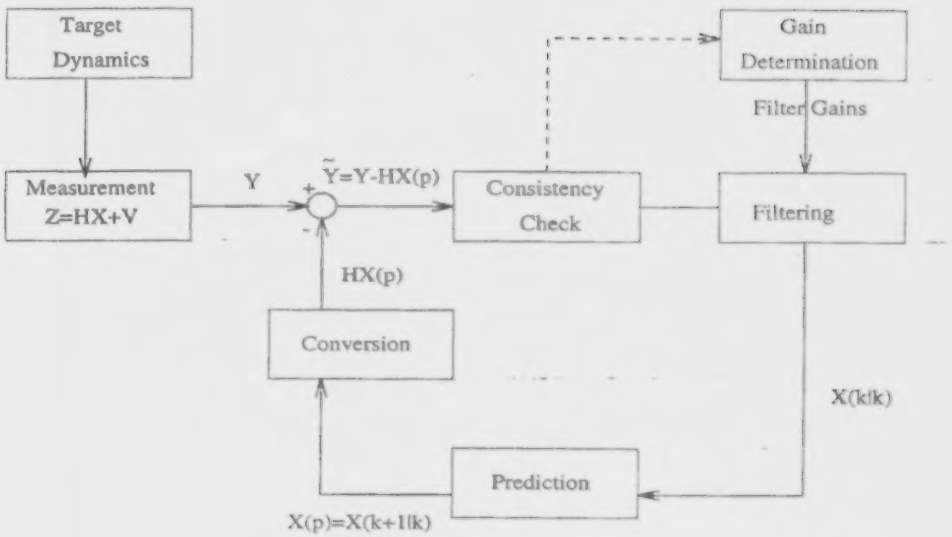

Figure 4.1: **Flow diagram of filtering and prediction**

measurement noise(v). The gains are used to provide filtered state estimates, which are then used to obtain estimate predicted to the next scan time. The residual process $\tilde{y}$ is the difference between the actual(z) and the expected measurement (Hx_p). This may be used to check the consistency for the Kalman filter gain.

The Kalman filter is the general solution for the recursive minimized mean square estimation problem within the class of linear estimators. Using of the Kalman filter will minimize the mean– square error as long as the target dynamics and the measurement noise are accurately modeled. In addition to minimizing the mean–square error, the Kalman filter has a number of other advantages for application to MTT. These advantages include:

1. The gain sequence is chosen automatically, based on the assumed target maneuver and measurement noise models. Therefore, the same filter can be used to different

P148588.PDF [Page: 29 of 83]

targets and environments by changing few key parameters.

2. The Kalman gain sequence automatically adapts to changing detection histories.
3. The Kalman filter provides a convenient measure of the estimation accuracy through the covariance matrix.
4. Through use of the Kalman filter it is possible to at least partially compensate for the effects of miscorrelation in the dense MTT environment.

The target dynamics process can be modeled in the discrete Markov form,

$$x(k+1) = \Phi x(k) + q(k) + f(k+1 \mid k) \tag{4.1}$$

where x is the n–dimensional target state vector that includes the quantities to be estimated. Φ is the assumed known transition matrix; $q(k)$ is the zero–mean, white, Gaussian noise with assumed known covariance Q; and $f(k+1 \mid k)$ is a known deterministic input, such as the relative position changing associate with own–ship position.

Measurements are in the form of linear combinations of the system state variables, corrupted by uncorrelated noise. Thus, the M–dimensional measurement vector is modeled as,

$$z(k) = Hx(k) + v(k) \tag{4.2}$$

where H is the M×N measurement matrix and $v(k)$ is zero–mean, white, Gaussian measurement noise with covariance R_c.

Given the target dynamics and measurement models from previous, the Kalman filter for MTT becomes

P148588.PDF [Page: 30 of 88]

$$\hat{x}(k \mid k) = \hat{x}(k \mid k-1) + K(k)[z(k) - H\hat{x}(k \mid k-1)] \tag{4.3}$$

$$K(k) = P(k \mid k-1)H^T[HP(k \mid k-1)H^T + R_c]^{-1} \tag{4.4}$$

$$P(k \mid k) = [I - K(k)H]P(k \mid k-1) \tag{4.5}$$

$$\hat{x}(k+1 \mid k) = \Phi\hat{x}(k \mid k) \tag{4.6}$$

$$P(k+1 \mid k) = \Phi P(k \mid k)\Phi^T + Q \tag{4.7}$$

and the vector difference between a measured and predicted quantities, $\tilde{y}(k) = z(k) - H\hat{x}(k \mid k-1)$, is defined to be the residual vector with residual covariance matrix, $S = HPH^T + R_C$.

The above statements and equations are the basic ideas about Kalman filtering in the MTT system. Before we implement the filtering, we need to specify the coordinates. There are two kinds of coordinate systems that are usually used in the MTT system. One is the Cartesian system and the other is the polar system. Tracking in Cartesian system has the advantage of allowing the use of linear target dynamic models for extrapolation. The target position prediction, such as x, can be computed from the simple linear equation,

$$X(k) = X(k-1) + v_x(k)T + \frac{1}{2}a_xT^2. \tag{4.8}$$

P148588.PDF [Page: 31 of 88]

In the polar system, this may lead to more complicated extrapolation.

However, the using of Cartesian coordinate also have two disadvantage. The first is that the measured range must be available in order to transform the measurements to the Cartesian coordinate. The second disadvantage is that the measurement errors are coupled, which are derived as follows. The measurements from $\rho-\theta$ space are transformed into $X-Y$ coordinate by

$$X_0 = R_0 \cos \eta_0, \qquad Y_0 = R_0 \sin \eta 0 \tag{4.9}$$

The measurement covariance matrix is

$$R_C = \begin{bmatrix} \delta^2_{x_0} & \delta^2_{x_0 y_0} \\ \delta^2_{x_0 y_0} & \delta^2_{x_0} \end{bmatrix} \tag{4.10}$$

where, using a first order expansion

$$\delta^2_{x_0} = \delta^2_{R_0} \cos^2 \eta + R^2 \sin^2 \eta \delta^2_{\eta_0} \tag{4.11}$$

$$\delta^2_{y_0} = \delta^2_{R_0} \sin^2 \eta + R^2 \cos^2 \eta \delta^2_{\eta_0} \tag{4.12}$$

$$\delta_{x_0 y_0} = \frac{1}{2} \sin 2\eta [\delta^2_{R_0} - R^2 \delta^2_{\eta_0}] \tag{4.13}$$

$\delta^2_{R_0}$, δ_{η_0} = range and azimuth angle measurement variances respectively. Unlike the polar system which only has two non–zero elements, this Cartesian coordinate system covariance matrix has four non–zero element. The four element is also changing with range and azimuth of a target.

P148588.PDF [Page: 32 of 88]

In our tracking system, we choose to use the Cartesian coordinate system. It is clear that the element of XY covariance matrix given by Eq. 4.11–4.13, is closely related to the range and azimuth position of target. Thus, at every scan, every element of the covariance matrix has to be updated.

P148588.PDF [Page: 33 of 88]

Chapter 5

Data Association

Data association is the essential part in the MTT problem. It is the process of assigning measurements to existing tracks for updating the tracks. Even though there are a lot of data association algorithms for the MTT fundamentally, there are two different models upon which data association algorithms can be constructed. The first model is a deterministic model, whose origin is certain or is so assumed for convenience, i.e.,

1. One takes the most likely of several "candidates " associations and ignores the fact that it is not necessarily correct, or
2. One carries out classical hypothesis testing, accepting the association hypothesis subject to a probability of error but then treating it as if it were certain.

The results of the deterministic association are then used in a standard state estimation algorithm — a linear or extended (linearized) Kalman filter.

P148588.PDF [Page: 34 of 88]

The second model is a probabilistic model, utilizing a Bayesian framework in which the probabilities of individual events (e.g., measurement 1 belongs to B) are computed and used in suitably modified state estimation algorithms.

The simplest approach of deterministic data association algorithm for tracking targets in a cluttered environment is the Nearest Neighbor algorithm which selects the validated measurement that is closest to the predicted measurement and use it in the tracking filter as if it were the correct one. This is an easy and fast algorithm but suffers in tracking close spacing targets. It may lose the tracks in high clutter because in high clutter environment, tracks are more possible to be associated with clutters if only nearest neighbor is used. Therefore, this is not the approach in our MTT system, although comparison between nearest neighbor and the PDA will be given later.

Another approach that handles the problem of simultaneously processing several measurements that could have originated from the target of interest is to split the track into multiple hypothesis every time when more than one measurement is found in the validation region. A "pruning' technique based on the likelihood function can be applied to reduce the number of false tracks. Nevertheless, the number of tracks can become too large in a dense environment. This is not the algorithm in our MTT system either.

One of the Bayesian approaches called Probability Data Association is the algorithm that we choose for our system. It deals with the latest set of validated measurement. It computes the probabilities of being correct for each validated measurement at the correct time. All the "neighbors " are probabilistically associated with the target of interest. Then

P148588.PDF [Page: 35 of 88]

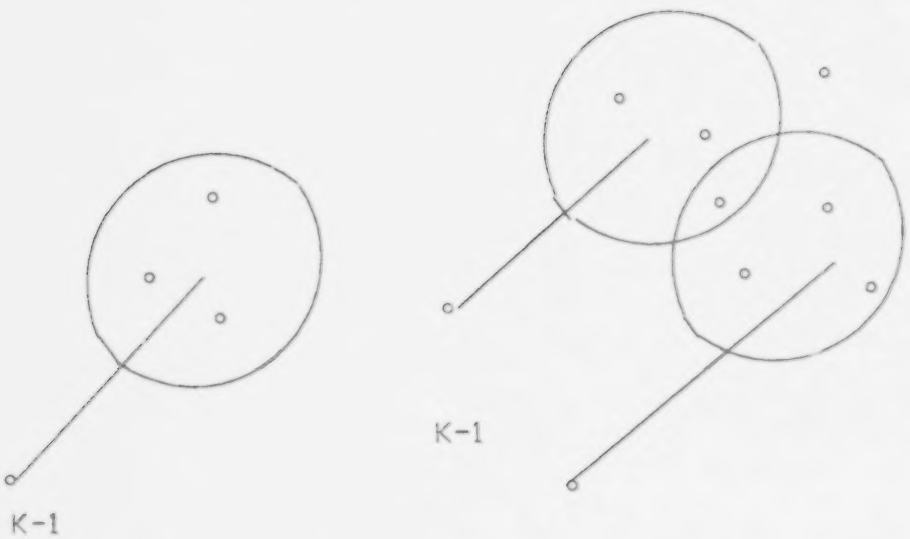

Figure 5.1: **Illustration of data association**

this probabilistic information is used in a suitably modified tracking filter, that accounts for the measurement origin uncertainty.

The probabilistic data association filter (PDAF) is a suboptimal Bayesian algorithm for those tracks that have been initialized. It is assumed that there is only one target of interest. For MTT case, the tracks and noise are assumed to be independent to one another in different validated measurement. Therefore, we use the PDAF for every different track.

At each sampling time a validation region is set up. Among the several possible validated measurements, one can be target originated and the remaining measurements are assumed to be false alarm or "residual clutter" modeled as independent identically distributed random variables with uniform spatial distribution.

P148588.PDF [Page: 36 of 88]

The set of validated measurements at time k is denoted

$$Z(k) \triangleq \{z_i(k)_{j=1}^{m_k}\} \tag{5.1}$$

where m_k (also a random variable) is the number of measurement in the validation region. If $m_k = 0$ (no detections fall inside the gate), then the set $Z(k)$ is empty. The cumulative set of validated measurements up to time k is

$$Z^k \triangleq \{z(j)_{j=1}^{k}\} \tag{5.2}$$

The center of the data association is to associate each validated measurement with appropriate target or to discard it as arising from clutter or false alarms.

The PDAF decomposed the estimation with respect to the origin of each element of the all test set of measurements. In order to carry out a decomposition with respect to the latest measurements only, the past is summarized approximately by making the following basic assumption of the PDAF,

$$P(x(k) \mid Z^{k-1}) = N[x(k); \hat{x}(k \mid k-1), P(k \mid k-1)] \tag{5.3}$$

i.e., the state is assumed to be normally distributed (Gaussian) according to the latest estimation and covariance matrix.

Following assumption of Eq. 5.3, $Z(k)$ contains measurements from the elliptical validation region $d(k)$ defined by Eq. 3.4. Define the events:

$\theta_i(k) \triangleq \{Z_i(k)$ is the target-originated measurement $\}$, i=1, ... , m_k

$\theta_0(k) \triangleq$ { none of the measurements at k is target—originated } with probabilities $\beta_i(k) \triangleq P\{\theta_i(k) \mid Z^k\}, i = 0, 1, ..., m_k$ conditioned on Z^k. In view of the above assumptions, these

P148588.PDF [Page: 37 of 88]

events are mutually exclusive and exhaustive, and hence

$$\sum_{i=0}^{m_k} \beta_i(k) = 1 \tag{5.4}$$

Using the total probability theorem with respect to the above events, the conditional mean of the state at time k can be written as,

$$\begin{aligned} \hat{x}(k \mid k) &= E[x(k) \mid Z^k] && (5.5)\\ &= \sum_{i=0}^{m_k} E[x(k) \mid \theta_i(k), Z^k] P\{\theta_i(k) \mid Z^k\} && (5.6)\\ &= \sum_{i=0}^{m_k} \hat{x}_i(k \mid k)\beta_i(k) && (5.7) \end{aligned}$$

where $\hat{x}(k)$ is the updated state estimate conditioned on the event $\theta_i(k)$ that the i*th* validated measurement is correct. $\hat{x}_i(k \mid k)$ is the Kalman filter output given by $\hat{x}_i(k \mid k) = \hat{x}(k \mid k-1) + K(k)\tilde{y}_i(k)$ i=1, ..., m_k

where $\tilde{y}_i(k) \triangleq z_i(k) - x(k \mid k-1)$ is the corresponding innovation. The gain $K(k)$ is the same as in the standard filter Eq. 4.4. For i=0, i.e., if none of the measurement is within the validated region, the estimate is

$$\hat{x}_0(k \mid k) = \hat{x}(k \mid k-1) \tag{5.8}$$

If we introduce the

$$v(k) \triangleq \sum_{i=1}^{m_k} \beta_i(k)\tilde{y}_i(k)$$

as the combined innovation, the state update equation of the PDAF can be expressed as

$$\hat{x}(k \mid k) = \hat{x}(k \mid k-1) + K(k)v(k) \tag{5.9}$$

P148588.PDF [Page: 38 of 88]

The error covariance associated with the updated state estimate is

$$P(k \mid k) = \beta_0 P(k \mid k-1) + [1 - \beta_0(k)]P^c(k \mid k) + \tilde{P}(k) \tag{5.10}$$

where

$$\tilde{P}(k) = K(k)\{\sum_{i=1}^{m_k} \beta_i v_i(k) v_i'(k) - v(k)v'(k)\}K'(k) \tag{5.11}$$

and

$$P^c(k \mid k) \triangleq [1 - K(k)H(k)]P(k \mid k-1) \tag{5.12}$$

Evaluation of the association probabilities is carried out as follows. First the conditioning is known down into the past data Z^{k-1} and the latest data, which consist of m_k measurement at locations $Z_1(k), ..., Z_{m_k}(k)$. Since a probabilistic inference can be made on the number of measurements in the validation region, this can be written as,

$$\beta_i(k) \triangleq P(\theta_i(k) \mid Z^k) \tag{5.13}$$

$$= P(\theta_i(i) \mid Z(k), m_k, Z^{k-1}), \quad i = 0, 1, ..., m_k \tag{5.14}$$

Using Bayesian rule, this may be written as

$$\beta_i(k) = \frac{1}{C} P[Z(k) \mid \theta_i(k), m_k, Z^{k-1}] P[\theta_i(k) \mid m_k, Z^{k-1}] \qquad i = 0, 1, ..., m_k \tag{5.15}$$

where C is the normalized constant.

The joint density of the validated measurements conditioned on $\theta_i(k), i \neq 0$ is the product of the (assumed) normal PDF of the correct (target–originated) measurement and the uniform PDF of the incorrect measurements. The clutters are assumed uniformly and independently distributed in the validation region.

P148588.PDF [Page: 39 of 88]

The PDF of the correct measurement is

$$P[Z_i(k) \mid \theta_i(k), m_k, Z^k] = P_G^{-1} N[Z_i(k); \hat{Z}(k \mid k-1), s(k)] \quad (5.16)$$

$$= P_G^{-1} N[\tilde{y}_i(k); 0, s(k)] \quad (5.17)$$

$$= P_G^{-1} \mid 2\pi S(k)) \mid^{\frac{1}{2}} exp[-\frac{1}{2}\tilde{y}_i' S^{-1}(k)\tilde{y}_i(k)] \quad (5.18)$$

where P_G is the gate probability, then the PDF from Eq. 5.15 is

$$P[Z(k) \mid \theta_i(k), m_k, Z^{k-1}] = \begin{cases} V_k^{-m_k} P_G^{-1} N[\tilde{y}_i(k); 0, S(k)] & i = 1, ..., m_k \\ V_k^{-m_k}, & i = 0 \end{cases} \quad (5.19)$$

where V_k is the volume of the validation region.

An important feature of the PDAF is that its computational requirements are the same as the standard filter's when only one return falls in the window and increase slightly when the need of processing multiple returns arises. Based on a computer instruction count, Table. 5.1 shows the approximate increase of the computational requirements of PDAF compared to the standard filter as a function of the number of returns in the validation region.

Number of Validated Returns	1	2	3	4
Factor of Increase	1	1.4	1.6	1.8

Table 5.1. Computational requirement comparison between Nearest Neighbor and Probability Data Association

Chapter 6

Direction weighting data Association

In this chapter, direction weighting is incorporated into the probabilities of probability data association for the measurement–track parings assignment. First, we would like to introduce some basic concept about the motion perception.

Direction weighting is based on the nature of motion perception. There are two types of motion perception: real motion and apparent motion. Real motion is perception elicited by actual movement of an object: (1) an image of an object moving across the retina or (2) an image of an object stationary on the retina but motion sensation from eye pursuit movement. Apparent motion perception is an induced visual illusion caused by temporal variation of stimulus even though both eye and its retina remain stationary. This is quite similar to the case of radar screen return spots, the aspect of apparent motion is examined here.

Depending on the time duration, separation distance and intensity, we can perceive move-

P148588.PDF [Page: 41 of 88]

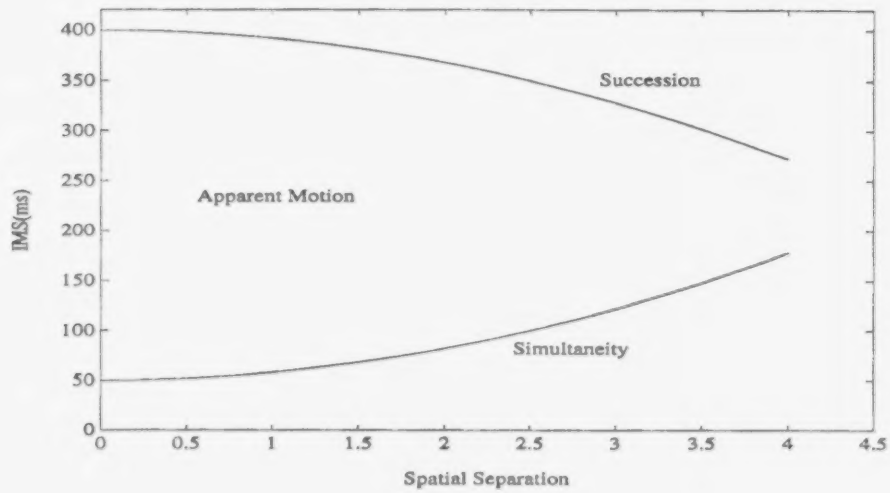

Figure 6.1: **Condition to generate apparent motion perception**

ment of light crossing among the two spots. As shown in Fig. 6.1, when spatial frequency is long and inter–stimulus interval (ISI) is short, we perceive two simultaneous and continuous lights. However, if ISI is long, then two lights blink alternatively at the two positions. While under other conditions, we will perceive crossing movements of a light.

As the light turns on and off, the input stimulus is stored and dissipated in the sensor memory as time elapses. In space, propagation of sensation can be modeled by a Gaussian waveform, thus the response of neighboring cells is expressed as follows,

$$G_{ij} = Cexp[\frac{-(j-i)^2}{2\delta^2}] \tag{6.1}$$

and the motion signal at the position i is then a sum of all responses from the neighboring

P148588.PDF [Page: 42 of 88]

cells, which are amplitude modulated Gaussian waveforms expressed in equation,

$$M_i = \sum_i x_i G_{ij} \tag{6.2}$$

Therefore, when amplitude–modulated Gaussian waveforms are overlapped, a trace of ridge between the two light position can be generated.

Various experiments on perception based association that occurs during apparent motion perception have been tabulated in Fig. 6.2. In the Fig. 6.2, the solid line indicates the object displayed in the first frame and the dashed line is from the second frame.

First, the original line prefers the closer occurrence. When two occurrences are the same distance to the original line, the preferred direction of apparent motion is toward the figures with similar attributes, such as direction, length, luminance, and topology. Also, as show in Fig. 6.2, the perceived motion favors more the direction acquired from the past experience than the correct figural proximity. All those show that the perception based association is based on proximity, attribute affinity and learning, the same principles as those employed in classical data association techniques.

In the problem of tracking, direction is one of the most important parameter determining the potential movement of tracks. Therefore, we modify PDA algorithm by including a direction attribute. This direction attribute adds a direction weighting function in the probability of PDA, which weights most the co–linear direction.

When we add direction weighting to probability of PDA, pseudo direction must be introduced since the direction information is not directly measurable. The pseudo direction is

P148588.PDF [Page: 43 of 88]

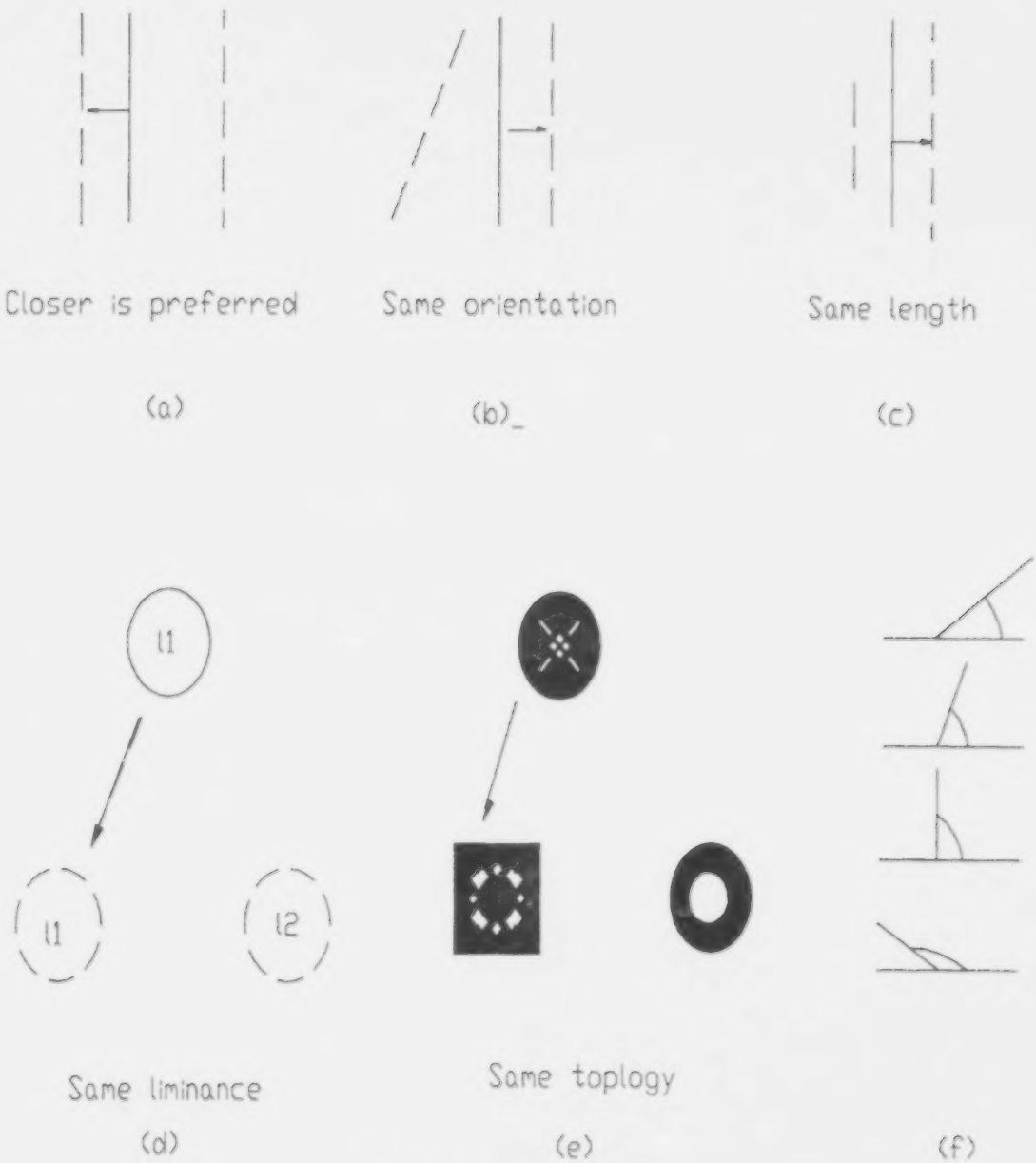

Figure 6.2: Perception based association during apparent motion

P148588.PDF [Page: 44 of 88]

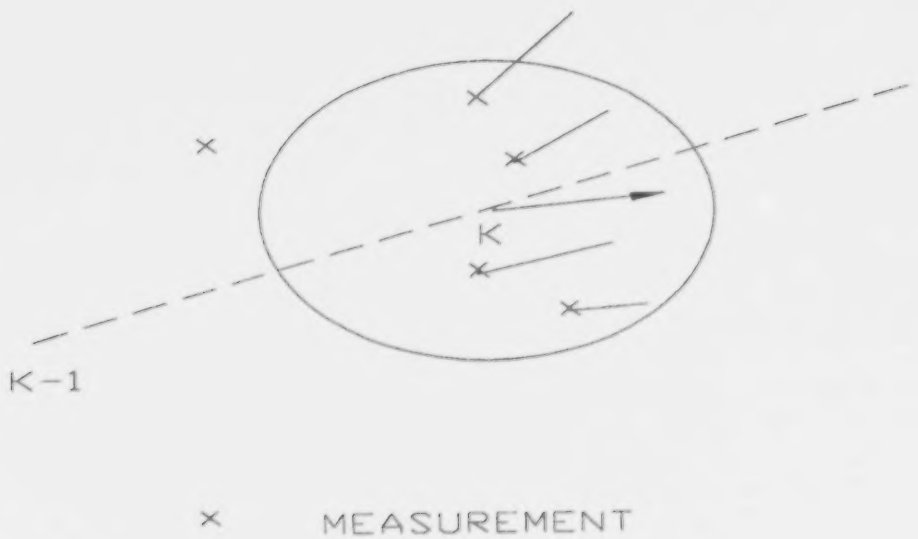

Figure 6.3: **Generation pseudo direction**

computed using the prediction information. Then, by connecting the validate measurement points with the previously predicted target position, $\hat{x}(k-1 \mid k-2)$, we can get the information of direction measurement. After that, we use the angle difference between the pseudo direction and predicted direction at the kth scan to determine the direction weighting. If Gaussian weighting is used, $exp(\frac{\Delta_{ij}^T \sigma_\Phi^{-1} \Delta_{ij}}{2})$ is added to the probability of PDA. σ_Φ is the variance of target heading. It is derived as follow:

Given a four state track vector, $\hat{X}(k) = [\hat{x}, \hat{x}', \hat{y}, \hat{y}']$ then the target heading and speed is

defined as,

$$\Phi = \tan^{-1} \frac{y'}{x'} \tag{6.3}$$

P148588.PDF [Page: 45 of 88]

$$v = \sqrt{(x')^2 + (y')^2} \tag{6.4}$$

The first and the second moments can be computed by using the linearization method, assuming the high order terms can be neglected.

$$\Delta\Phi = \frac{\partial\Phi}{\partial x'}\Delta x + \frac{\partial\Phi}{\partial y'}\Delta y + O(\Delta x^2, \Delta y^2, \Delta x\Delta) \tag{6.5}$$

By differentiating Eq. 6.3, we get

$$\frac{\partial\Phi}{\partial x'} = -\frac{y'}{v^2}, \qquad \frac{\partial\Phi}{\partial y'} = \frac{x'}{v^2} \tag{6.6}$$

the approximately, we get

$$\Delta\Phi = \frac{-y'}{v^2}\Delta x' + \frac{x'}{v^2}\Delta y' \tag{6.7}$$

Computing the expectation and the variance from Eq. 6.7 resulting in

$$E\{\Delta\Phi\} = \frac{1}{v^2}\{-y'E[\Delta x' + x'E[\Delta y']\} = 0 \tag{6.8}$$

$$E\{(\Delta\Phi)^2\} = \sigma_\Phi^2 \tag{6.9}$$

$$= \frac{[(y')^2 P_{x'} - 2x'y'P_{x'y'} + (x^2)^2 P_{y'}]}{v^4} \tag{6.10}$$

where the covariance terms are from,

$$P(k) = \begin{bmatrix} P_x & P_{xy} & P_{xx'} & P_{xy'} \\ P_{xy} & P_y & P_{yx'} & P_{yy'} \\ P_{x'x} & P_{x'y} & P_{x'} & P_{x'y'} \\ P_{xy'} & P_{xy'} & P_{x'y'} & P_{y'} \end{bmatrix} \tag{6.11}$$

P148588.PDF [Page: 46 of 88]

Since in our system, only the range and azimuth measurements are available, the variance of x' and y' is derived from the variance of x and y.

Using real data and simulated data, we compare the performance between the Nearest Neighbor, Direction weighting Probability Data Association and Probability Data Association.

First, we use the simulated data to compare the performance of these three methods.

In Table. 6.1 are given track outputs obtained using nearest neighbor data association and probability data association. Nineteen scan data are used to obtain these results. In the table, the *No. of scan* stands for the starting point of the track, e.g., that *No. of scan* is equal to 3 means the track starts at the 3rd scan. Track deletion logic is not carried here. Therefore at every scan, a new track is initiated. From Table. 6.1, it is seen that the track initiated at the first scan will only have a length of 14 using nearest neighbor while the length of track is 19 for probability data association. This is because the nearest neighbor only takes the local information into consideration and this will result in losing tracks.

In Fig. 6.4 and Fig. 6.5 are shown the performance comparison, in terms of the percentage of track loss, between the data association techniques. The percentage of track loss is defined as

$$p_l = \frac{N_l}{N_t} \tag{6.12}$$

where N_l and N_t are the total number of lost tracks and the total number of existing tracks.

In Fig. 6.4, the percentage of track loss is compared at different mean values of clutters to real returns ratio per scan. The clutters to real return ratio per scan is given by Eq. 2.10.

P148588.PDF [Page: 47 of 88]

Table 6.1: **Two data file of the length of tracks using probability data association and nearest neighbor**

PDA(DPDA)		Nearest Neighbor	
No. of scan	Length of Track	No. of scan	Length of Track
1	19	1	14
2	18	2	13
3	17	3	12
4	16	4	11
5	15	5	10
6	14	6	9
7	13	7	8
8	7	8	7
8	12	8	12
9	11	9	11
9	11	9	11
10	10	10	10
10	10	10	10
11	9	11	9
11	9	11	9
12	8	12	8
12	8	12	8
13	7	13	7
14	6	14	6

P148588.PDF [Page: 48 of 88]

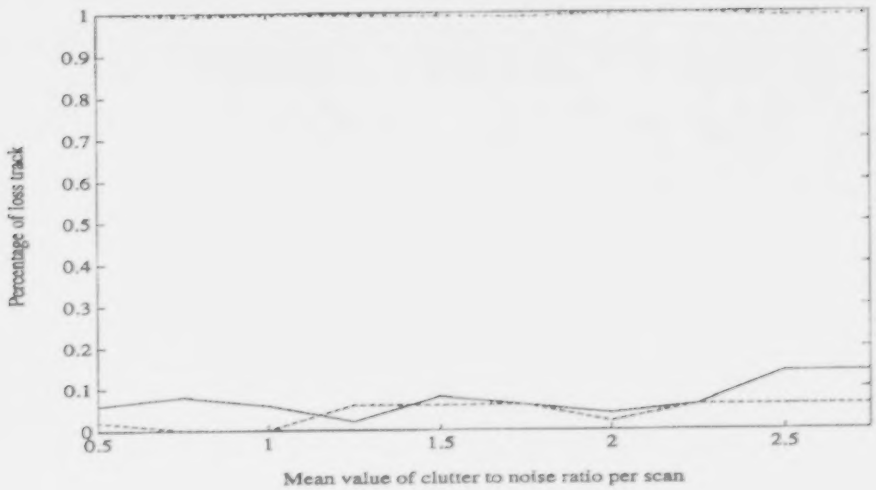

Figure 6.4: **Percentage of track loss in clutter environment. — PDA - - DPDA -.- NN**

The number of clutters per scan is generated randomly with a Poisson distribution. The distribution of the clutter in per scan is uniformly distributed. Each value of p_l in the figure is obtained using 500 trails. In Fig. 6.5, the percentage of track loss is compared at different noise level. The measurement noise is assumed to be normal distribution. Each value of p_l in the figure is also obtained using 500 trails. The result show that the probability data association algorithm are superior to the nearest neighbor technique in te m of percentage of track loss.

Real data are also analyzed using DPDA, PDA and NN. Part of the LAB data are used to compare the tracking by three methods. The results are shown in Fig. 6.6 to Fig. 6.8. From the figures, we can see PDA estimation may be bit from measurements while the nearest neighbor always sticks on the measurement.

P148588.PDF [Page: 49 of 88]

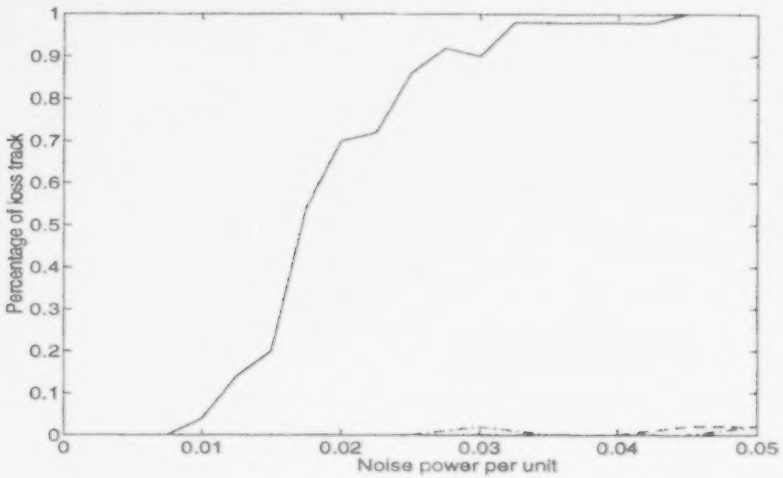

Figure 6.5: **Percentage of track loss in different noise environment — Nearest Neighbor - - PDA -. DPDA**

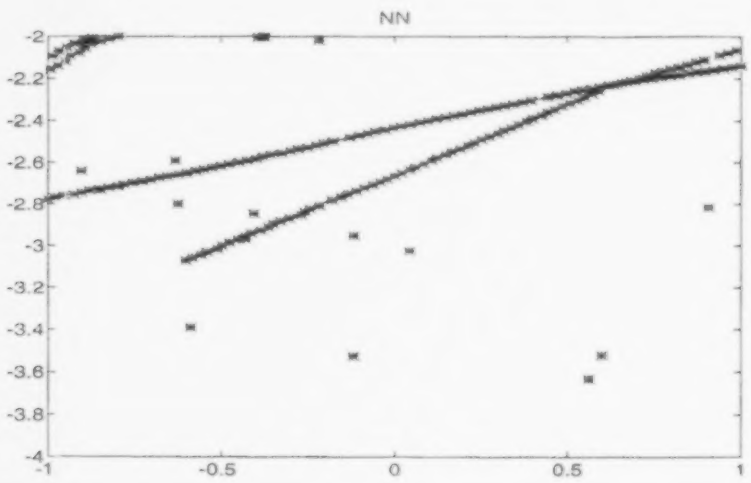

Figure 6.6: **Tracking real data using standard nearest neighbor algorithm**

P148588.PDF [Page: 50 of 88]

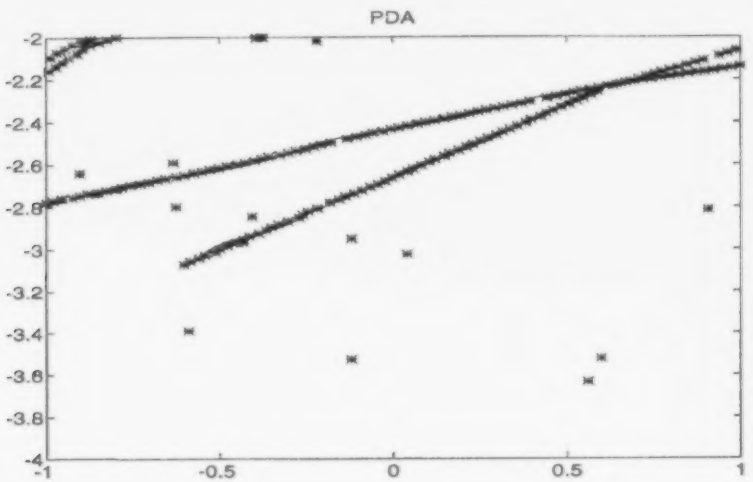

Figure 6.7: **Tracking real data using Probability Data Association algorithm**

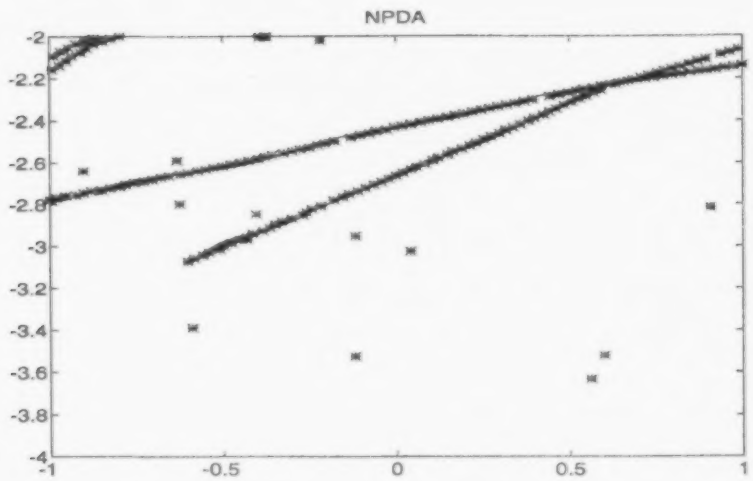

Figure 6.8: **Tracking real data using Direction weighting Probability Data Association algorithm**

P148588.PDF [Page: 51 of 88]

Table 6.2: **Comparison between the number of tracks with direction weighting and without direction weighting**

File name:	Without Direction Weighting (No. of Track)	With Direction Weighting (No. of tracks)
rt11	7051	2571
rt12	2673	311
rt1322	351	706
rt134	985	1413
rt141	9435	1964
rt11421	9799	880

Another advantage of using DPDA is that DPDA reduces the multiple initiated tracks, which will be discussed in chapter 8. Here, we just give a table shows that with the same type of tracking accuracy, the DPDA reduces the number of tracks that have been tracked.

We can see from the table, generally the DPDA recudes the number of tracks that have to be tracked because it gives more accurate estimation than the PDA. Thus it is less likely to lose the track. However, as we see from Table. 6.2, the DPDA may have more tracks to be followed. This is the case when target is maneuvering.

P148588.PDF [Page: 52 of 88]

Chapter 7

Neural Network for Data Association

Data association in multiple target tracking is very similar to the classical problem called Traveling Salesman Problem (TSP). For this reason, many kinds of neural networks that have been successfully used to solve TSP are introduced for the MTT problem, such as Hopfield network, Boltzmann machine. These networks make use of the connection strength which can be obtained from the distances between measurements and predicted position to find the optimal path of assignment. In this chapter, we first give a brief review of Traveling Salesman Problem and then implement the Hopfield network and Boltzmann machine for data association.

7.1 Traveling Salesman Problem (TSP)

The Traveling Salesman Problem (TSP) is to find the minimal path for a traveling salesman to visit each city exactly once. It can be formulated as follow. We are given n cities and

P148588.PDF [Page: 53 of 88]

an $n \times n$ matrix $[d_{ij}]$, whose elements denote the distance between each pair p, q of the n cities. A *tour* is defined as a closed path visiting each city exactly once. The problem is to find a tour of minimal length. For this problem a solution is given by a cuclic permutation $\pi = (\pi(1), \cdots, \pi(n))$, where $\pi(k)$ denotes the successor city of city k, with $\pi^l(k) \neq k, l = 1, \cdots, n-1$ and $\pi^n(k) = k$, for all k. Each solution then corresponds uniquely to a tour. The solution space is given by

$$S = \{ \text{ all cuclic permutations } \pi \text{ on n cities } \} \tag{7.1}$$

The cost function is defined as

$$f(\pi) = \sum_{i=1}^{n} d_{i,\pi(i)}, \tag{7.2}$$

i.e. $f(\pi)$ gives the length of the tour corresponding to π. Furthermore, we have totally number of search $\mid S \mid = (n-1)!$. Fig. 7.1 is a typical traveling salesman problem. The solid line shows the best path while other types of line stand for part of the possible choice.

7.2 Hopfield Neural Network for the Data Association in Multiple Target Tracking

Data association for MTT is similar to the problem of Traveling Salesman wherein the minimal value for cost function is to be found by optimizing the assignment. Since Hopfield neural network has been successfully used to find the optimal solution for TSP, it is also attempted to solve the data association in MTT. Suppose there are n targets and m measurements. They are arranged in the matrix form as shown in Fig. 7.2. Each element in the

P148588.PDF [Page: 54 of 88]

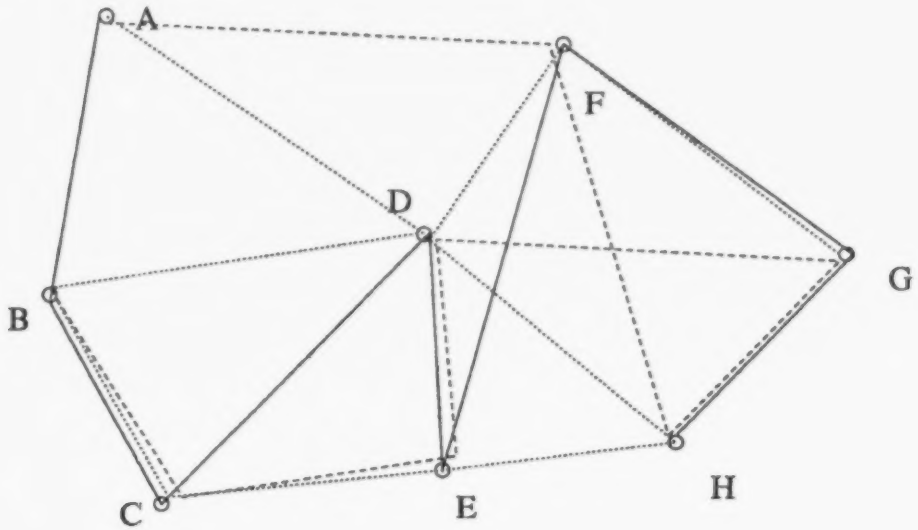

Figure 7.1: Typical problem of TSP

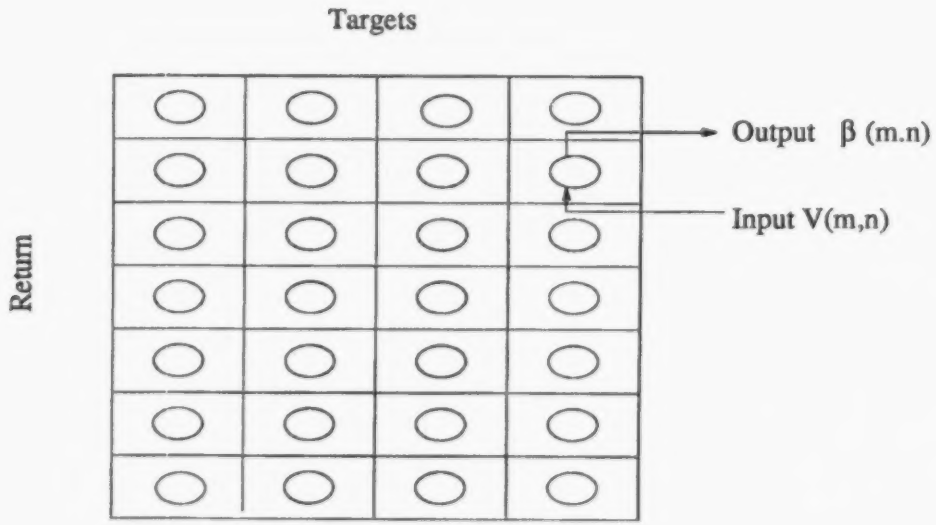

Figure 7.2: Array of interconnected neurons with input currents and output voltage

P148588.PDF [Page: 55 of 88]

matrix stands for the probability that the ith measurement is originated from the jth target. Iltis proposed a method of obtaining the probabilities for JPDA by using Hopfield neural network. The energy function for data association is proposed as

$$\begin{aligned} E_{DAP} &= \frac{A}{2}\sum_{j=0}^{m}\sum_{t=1}^{n}\sum_{\substack{\tau=1\\ \tau\neq t}}^{n} V_j^t V_j^t + \frac{B}{2}\sum_{t=1}^{n}\sum_{j=0}^{m}\sum_{\substack{l=0\\ l\neq j}}^{m} V_j^t V_l^t \\ &+\frac{C}{2}\sum_{t=1}^{n}(\sum_{j=0}^{m} V_j^t - 1)^2 + \frac{D}{2}\sum_{t=1}^{m}\sum_{t=1}^{n}(V_j^t - \rho_j^t)^2 \\ &+\frac{E}{2}\sum_{j=0}^{m}\sum_{t=1}^{n}\sum_{\substack{\tau=1\\ \tau\neq t}}^{n}(V_j^t - \sum_{\substack{l=0\\ l\neq j}}^{m}\rho_l^\tau)^2 \end{aligned} \tag{7.3}$$

where $V_{Y,0}$ is set to $V_{Y,n}$ and $V_{Y,n+1}$ is set to $V_{Y,1}$. The first three terms represent the constraints. The first term achieves its minimum value of 0 when there is at most one 1 in each row. The second term is minimized when there is at most one 1 in each column. The third term is expected to be force to total number of cities in the optimum tour to n. The fourth term represents the length of the tour which has to be minimized.

The evolution of Hopfield network is characterized by the following equations:

$$V_l^t = g(u_l^t) \tag{7.4}$$

$$\begin{aligned} \frac{du_l^t}{ds} &= \frac{u_l^t}{s_0} - A\sum_{\substack{\tau=1\\ \tau\neq l}}^{T} V_l^\tau - B\sum_{\substack{j=0\\ j\neq l}}^{m(k)} V_j^t - C(\sum_{j=0}^{m(k)} V_j^t - 1) \\ &-[D + E(T-1)]V_l^t + (D+E)\rho_l^t \\ &E(T - 1 - \sum_{\tau=1}^{T}\rho_l^\tau) \end{aligned} \tag{7.5}$$

The coefficients A, B, C, D and E can be adjusted to control the emphasis on different constraints and properties. A large value of D will produce V_l^t close to ρ_l^t which are approx-

P148588.PDF [Page: 56 of 88]

imately the ordinary PDA association probabilities. A larger emphasis on A, B, and C will produce the nearest neighbor solution. Thus, we can change the value of A, B, C, D and E to achieve different data association approximation.

The function $g(u_l^t)$ in above equation is defined

$$V_l^t = g(u_l^t) = \frac{1}{2}(1 + tanh\frac{u_l^t}{u_0}) \tag{7.6}$$

The inverse of this relation is

$$u_l^t = \frac{u_0}{2} ln(\frac{V_l^t}{1 - V_l^t}) \tag{7.7}$$

From the above Eq. 7.5, the differential equation is approximated by a difference equation

$$\begin{aligned} u_l^t(i+1) &= (\frac{s_0 - \zeta}{s_0})u_l^t(i) - \zeta A \sum_{\substack{\tau=1 \\ \tau \neq t}}^{T} V_l^\tau(i) \\ &\quad -\zeta B \sum_{\substack{j=0 \\ j \neq l}}^{m(k)} V_j^t(i) - \zeta C(\sum_{j=0} m(kV_j^t(i) - 1) \\ &\quad -\zeta[D + E(T-1)]V_l^t(i) + \zeta(D+E)\rho_l^t \\ &\quad +\zeta(T - 1 - \sum_{\tau} T\rho_l^t) \end{aligned} \tag{7.8}$$

s_0 and ζ were selected to be 1 s and 0.00001 s respectively. In the program developed, 400 iterations was imposed on the recursive equation. However, the experiment shows that this kind of network can converge quite fast. For small number of targets, we can reduce the number of iteration to 100. Fig. 7.3 is a typical output of the network.

It is well known that the Hopfield Neural Network may not approach the global minimal. Therefore, it is quite critical to assign the initial state to the network. In the previous literatures, there are two kinds of initial state assignment. One is to assign equal value to

P148588.PDF [Page: 57 of 88]

	Target 1	Target 2	Target 3	Target 4
No Return	0.01	0.02	0.01	0
Return 1	0.95	0	0	0
Return 2	0	0	0	0.93
Return 3	0	0.98	0.01	0.01
Return 4	0	0	0.96	0
Return 5	0.04	0	0.02	0.06

Figure 7.3: **A typical output of Hopfield neural network**

the initial state. Another possible choice of initial conditions is to assign the initial state as $V_i^t = \rho_i^t$ corresponding to initial measurement–to–track likelihoods. In our work, we use the direction weighting likelihoods as the initial state since this initial state is believed to be closer to the final optimized results. This may partially relief the problem of local optimal.

However, the above proposed neural network still have some problems for data association in multiple target tracking. First, the the connection strength seems not so reasonable. In the Hopfield Neural Network for Traveling Salesman Problem, the connection depends on the cities distance. In this issue, the connection strength is given

$$\begin{aligned} T_{ij}^{t\tau} &= -[A\delta_{ij}(1-\delta_{t\tau}) + B\delta_{t\tau}(1-\delta_{ij}) + C\delta_{t\tau} \\ &\quad + D\delta_{t\tau}\delta_{ij} + E(T-1)\delta_{t\tau}\delta_{ij}] \end{aligned} \tag{7.9}$$

It is observed that the connection is not depend on ρ_i^t. This is a kind of contradict to the

P148588.PDF [Page: 58 of 88]

Hopfield neural network for TSP. Since the ρ_i^t does not have effect on the connection strength, the optimization result may not influenced by the likelihoods. Thus, the data association result will mostly depend on the coefficient A, B, C, D, E selections. This is not the original idea of TSP.

It is believed that the above proposed Hopfield neural network energy function for data association is still premature to be implemented. The selection of coefficient A, B, C, D and E are kind of arbitrary, so it is almost impossible to implement this method into real system since in real system the number of target is always an unknown. The coefficient selected by Iltis's paper for 2–6 targets can not hold when the number of target is changing in a large scale.

7.3 Boltzmann machine and simulated annealing for data association

The Boltzmann machine was originally applied to pattern classification and learning was accomplished using gradient descent on the weights. Recently, various researchers have applied the Boltzmann machine to optimization problems such as the Traveling Salesman Problem, Max Cut Problem, Graph Coloring Problem and Independent Set Problem. In these research work, the TSP is closest to the data association problem in MTT, Following the same idea, the Boltzmann machine has been introduced in the MTT for optimization. Also, temperature is incorporated into the process of Boltzmann machine optimization as a

P148588.PDF [Page: 59 of 88]

control parameter. The whole process is combining the simulated annealing with Boltzmann machine. The general process of this work is as follow.

First, define a network with N^2 binary elements, $v(n,m) \in \{0,1\}$, and associated energy (consensus) function $E(v)$. Following the paper by Emile Aarts for TSP, a quadratic energy function is chosen as

$$E(v) = \sum_{n=1}^{N}\sum_{m=1}^{N}\sum_{n'=1}^{N}\sum_{m'=1}^{N} v(n,m)v(n',m')T_{n,m}^{n',m'} \tag{7.10}$$

In the above equation, the $T_{n,m}^{n',m'}$ is a scalar and presents interconnections between neurons $v(n,m)$ and $v(n',m')$. The goal of Boltzmann machine attempts to find a global minimum of $E(V)$ by performing simulated annealing to avoid convergence to local minima. On each iteration, the network picks a neuron $v(n,m)$ at random and attempts to change its state. If the resulting energy $E(V)$ decreases, the network will usually accept this transition. However, even if the change in state caused an increase in $E(V)$, the network will occasionally also accept the resulting transition. A suitable annealing achedule is selected to let the network climb out of local minima and eventually settles down to the global minimum.

The Boltzmann machine energy function proposed for the data association in MTT is chosen to be

$$\begin{aligned} E(V,T_a) &= \sum_{n=1}^{N}\sum_{m=1}^{N} v(n,m)\rho(n,m) \\ &\quad + \frac{A}{T_a}\sum_{n=1}^{N}\sum_{m=1}^{N}\sum_{k\neq m} v(n,m)v(n,k) \\ &\quad + \frac{B}{T_a}\sum_{m=1}^{N}(\sum_{n=1}^{N} v(n,m) - 1)^2 \end{aligned} \tag{7.11}$$

P148588.PDF [Page: 60 of 88]

The connection matrix $T_{n,m}^{n',m'}$ is

$$\begin{aligned} T_{n,m}^{n',m'} &= \rho(n,m)\delta_{n,n'}\delta_{m,m'} + \frac{A}{T_a}(1-\delta_{m,m'})\delta_{n,n'} \\ &\quad + \frac{B}{T_a}\delta_{m,m'} - \frac{2B}{T_a}\delta_{n,n'}\delta_{m,m'} \end{aligned} \tag{7.12}$$

where $\delta_{n,m}$ is the Kronecker delta. It is observed that the structure $T_{n,m}^{n',m'}$ is not fully interconnected. Rather, each neuron $v(n,m)$ is connected only to the remaining neurons in its column n and row m, thus greatly simplified implementation of the network. Unlikely the Hopfield neural network energy function in the previous section, this energy function does include the distance information into the connection strength. Furthermore the $\rho(n,m)$ in here represents the normalized Euclidean distance between measurement $z(n)$ and parameter $x(m)$, specifically

$$\rho(n,m) = \frac{(z(n)-x(m))^2}{2\delta_n^2} \tag{7.13}$$

The input output relationship of Boltzmann machine is characterized by the familiar sigmoid form

$$\begin{aligned} v_{n,m}(t) &= g(u_{n,m}(t)) \\ &= \frac{1}{1+e^{-\alpha u_{n,m}(t)}} \end{aligned} \tag{7.14}$$

An energy function $E_d(U)$ is then defined in terms of $E(V)$ by

$$E_d(U) = E(V)\,|_{v_{n,m}(t)=g(u_{n,m}(t))} \tag{7.15}$$

The neuron inputs, $u_{n,m}(t)$, propagate according to the following vector diffusion equation

P148588.PDF [Page: 61 of 88]

Measurements	Targets 1	2	3	4	5
0	0	0	0	0	1
1	1	0	0	0	0
2	0	1	0	0	0
3	0	0	0	1	0
4	0	0	0	0	0
5	0	0	1	0	0
6	0	0	0	0	0
7	0	0	0	0	0

Figure 7.4: **A valid Boltzmann machine configuration for computing the JPDA data association probabilities**

(Langevin equation)

$$du_{n,m}(t) = -\frac{dE_d(U)}{du_{n,m}(t)}dt + \sqrt{2}dw_{n,m}(t) \tag{7.16}$$

where $w_{n,m}(t)$ is the standard Wiener process. Substitution of the Boltzmann energy function into the Langevin equation yields the following equation of the n,mth amplifier input voltage

$$\begin{aligned}\frac{du_{n,m}(t)}{dt} &= \alpha v_{n,m}(t)(1 - v_{n,m}(t)) \\ &\quad (\sum_{n',m' \neq n,m} T_{n,m}^{n',m'} v(n',m') \\ &\quad + \sum_{n',m' \neq n,m} T_{n',m'}^{n,m} v(n',m') \\ &\quad + 2T_{n,m}^{n,m} v(n,m)) + n_w(t)\end{aligned} \tag{7.17}$$

where $n_w(t)$ is white Gaussian noise.

P148588.PDF [Page: 62 of 88]

The whole process of implementation Boltzmann machine for data association is generalized as the following steps

- Form a n by m matrix where the n and m is the number of targets and measurements respectively. Fill the matrix using either 1 or 0 randomly.
- Through Eq. 7.14 to evaluate the output of each neuron.
- Using Eq. 7.17 to evolute the neural network. Then use Eq. 7.14 again to get the new output. Do this process iteratively and the number of iteration is enforced to be 500.
- Cooling the temperature. Repeat the previous 3 processes again.
- Using M parallel machine to do all the previous processes simultaneously.
- Finally, the estimation of the association probabilities is given by

$$\hat{\beta}_i^j = \frac{1}{M} \sum_{m=1}^{M} v^m(i,j) \tag{7.18}$$

  where $v^m(i,j)$ indicates neuron $v(i,j)$ in the mth machine.

The parameter in the Boltzmann is selected as

- $\alpha = 100$.
- $A = B = 10$.
- The number of parallel machine is chosen to be $M = 20$.
- The temperature starts at 100 and decrease at a rate of 0.95 until it reaches 1.

P148588.PDF [Page: 63 of 88]

- The white Gaussian noise in Eq. 7.17 is not modeled in the equation. here

However, we find there are also some problems remained in using Boltzmann machine for data association. Some typical problems are:

1. Coefficients selection of neural network will have a large influence on the output of a neural network. In our implementation, we fixed all other coefficients of the network and choose different A and B to test the performance of the network. The input $\rho(n,m)$ is normalized to its maximum value. It is found that the network will give the best performance when A and $B \in \{5,15\}$ for 2 to 5 targets. When the coefficients are out of this range, the data association some times totally fails. Should we use different A and B coefficient under different number of target? More investigation is needed to answer this question.

2. The Iltis's paper[11] uses an incorrect idea to achieve the probabilities for joint probability data association. As is well known, the Boltzmann machine for TSP is try to find the minimal length path for the salesman among all the pathes. In data association for MTT, actually this is trying to find the global nearest neighbor. That is to say the summation of the normalized distances between targets and measurements is to be minimized. There is only one best assignment for each configuration. However, in the Iltis's paper using Boltzmann machine for data association, the author used the simple average of different parallel machines outpout to obtain the probabilities for data association. They included failure

P148588.PDF [Page: 64 of 88]

search into the probabilities for data association. In the paper, they compare the average output with the JPDA result and it looks that the results are very close. We think this is just coincidence.

3. The third difficulty of using Boltzmann machine for optimization is the sensitivity of the network to its input. In multiple target tracking, the problem is how sensitive the network is to the normalized distance $\rho(n,m)$. When the distances between a predicted position and some measurements are much smaller than the distances between the predicted position and other measurements, say the ratio of $\frac{1}{1000}$, our simulation shows that the Boltzmann machine may not always find the optimal association. Actually the probability of assigning the measurement with normalized distance at 0.2 to target is equal to the probability of assigning the measurement with normalized distance at 0.1. Referencing the Table II in Itlis's paper [11] on using Boltzmann machine for data association, at the top–left corner, the probabilities are very close. This means that the number of failure search is very close to the number of successed search. The sensativity analysis of the neural network for optimization is needed before it can be correctly implemented for data association in MTT.

4. Computation time is another concern in using the Boltzmann machine in MTT. In the paper[11], using Boltzmann machine for find the data association result when n=m, the total number of calculation is $n \times n \times 500 \times 90 \times 20$. JPDA exhaustive search need n! number of step search. In the simulation case where there are only

P148588.PDF [Page: 65 of 88]

four targets, Boltzmann machine is really more expensive.

5. The paper[11] claims that the the network accuracy of probability estimation will increase with the increase of number of parallel machine. However, it is questionable how accuracy is determined by the number of machines or by network itself. This needs to be investigated further.

   It might be a good idea to use neural network in multiple target tracking. However, the two previous papers[11] have some problems remained for implementation. More research is needed in this area.

P148588.PDF [Page: 66 of 88]

Chapter 8

Real Data and Simulation Test

Raid Tracking Trails (RATT) data are provided by the Defense Research Establishment Ottowa (DREO) to test the algorithm. The test data were gathered at Canadian force Base, Cold Lake, Alberta in September 1986. Six CF–18 fighter aircraft, flying prescribed routes in prescribed formations, served as "raid" targets. Scan by scan, the data is recorded.

Air traffic control radars manufactured by Westinghouse are used to collect the RATT data. The radar scans at the rate of 12/rpm. Beam width is 2°. Range probability of detection are 80 mile 80 % and 40 mile 90 % respectively. Range resolution is around 1000 feet since the radar flight returns are marginal resolvable when two target flying around this distance.

The variances of the target range and azimuth are set to be one third of the radar resolution and expressed in terms of the covariance matrix of x and y based on Eq. 4.10–4.13.

P148588.PDF [Page: 67 of 88]

Two practical techniques are used in the analysis:

1. Track Deletion

   There are two kinds of tracks should be deleted for computation purpose. One is the lost tracks. The lost tracks are caused by the clutter initiation and sharp acceleration of flights. As shown in Fig. 8.1(a), suppose we have a confirmed target at Position 1. Based on this position and estimated target dynamics, we get the next target position is predicted to be Position 2 indicted by a small rectangular. The shadow gate is formed around the predicted position. If there is no measurement within the gate, we continue the prediction using previous target dynamic information and apply an enlarged gate. It is obvious that it is not necessary to keep a track which has no measurement to be associated with for a number of scans. This leads to the question that how many steps is necessary to continue enlarging the gate and predicting? In our case, if a track can not be associated with any measurements for 4 consequent scans, the track is terminated.

   Another kind of tracks that should be deleted are the multiple initiated tracks as shown in Fig. 8.1(b). Since in a real system, targets may come into radar retina at any time, our initiation algorithm has to work at every scan adding new tracks to the track file. New initiated tracks may use the same measurements that have been used to update the existing tracks. These multiple initiated tracks should be deleted since it actually is the same tracks as the existing tracks. The multiple initiated tracks are deleted using spatial correlation. In our test, this can save

P148588.PDF [Page: 68 of 88]

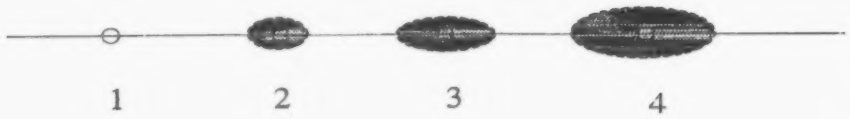

(a)

(b)

Figure 8.1: **Two kinds of tracks that should be deleted**

around 30 % of computation.

2. Window Technique

   At every scan, a lot of spatially separated measurements are collected. However for the speed limitation, not all the points are possible to be associated with tracks. In light of gating technique, we propose using divided windows to divide the whole region into a number of windows. Each of which is analyzed by at the same time. This reasonable approach provides a great advantage — great computation saving. Suppose we have n radar returns uniformly separated at every scan. If we set m equal windows, the number of returns in every window becomes $\frac{n}{m}$. When we use five scans to initiate a track without window, the initiation algorithm will associate all $2n^3$ possibilities. After we set the window, it will associate $(2\frac{n}{m})^3 \times m$ points.

P148588.PDF [Page: 69 of 88]

This will improve the speed by a factor of m^2 and almost the same accuracy. If we add more windows at the adjunct of previous window, same accuracy will be achieved while the speed can be improved by a factor of m^2.

The following is the tracking result using different data association algorithms.

Fig. 8.2–Fig. 8.4 show measurement returns R1T1 and tracking results using direction probability data association and Hopfield neural network implemented joint proability data association. Fig. 8.2 one is the original measured data. Fig. 8.3 is tracking results using direction PDA. Fig. 8.4 is the tracking results using Hopfield neural network implemented JPDA. Since the Hopfield neural network may leads to local minimum, the tracking results are not very satisfied.

Similarly, we plot the measured data (R1T2, R2T1, R2T2) and tracking results in Fig. 8.5–Fig. 8.11.

Fig. 8.12–Fig. 8.15 show tracking another set of real data (LAB) using developed multiple target tracking system. Fig. 8.12 is the measured data. Fig. 8.13 is the tracking result using nearest neighbor data association. Fig. 8.14 and Fig. 8.15 are the tracking results using PDA and direction PDA respectively. It can be seen from the figures that for the nearest neighbor data association, the number of false tracks increases in high clutter environment. The probability data association gives performance superior to the nearest neighbor data association in the clutter environment. However, Some thick lines which are caused by redundant track calculation appear. The direction weighting probability data association combines the advantages of previous two. It reduces the number of false tracks as well as

P148588.PDF [Page: 70 of 88]

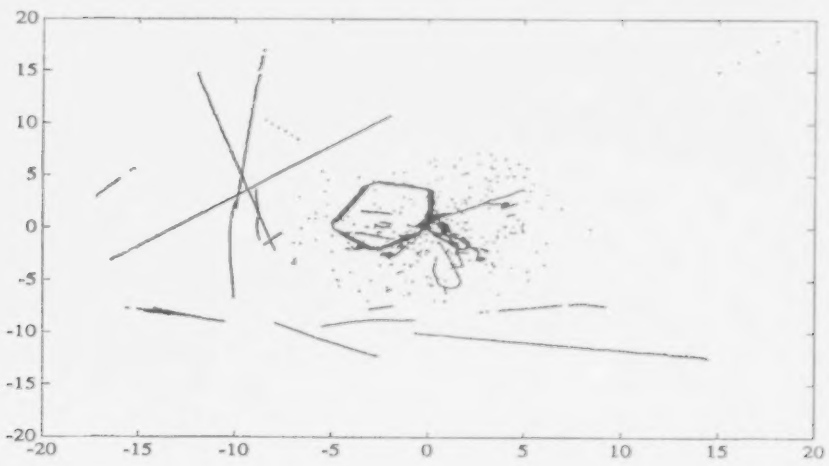

Figure 8.2: Measured data of R1T1.

the calculated tracks.

Fig. 8.16–Fig. 8.18 show the tracking results using Boltzmann machine implemented joint probability data association. From simulation results Fig. 8.16–Fig. 8.18, we can see that the Boltzmann machine implemented joint probability data association works fine for small number of target. However, with the increasing number of targets, the tracking accuracy will decrease. Since the current Boltzmann machine still have some problems remained, tracking real data result is not satisfied.

P148588.PDF [Page: 71 of 88]

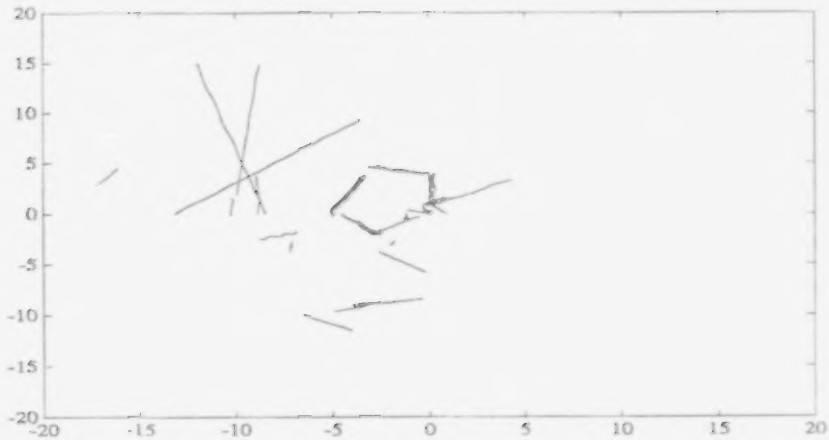

Figure 8.3: Tracking R1T1 data using direction probability data association

P148588.PDF [Page: 72 of 88]

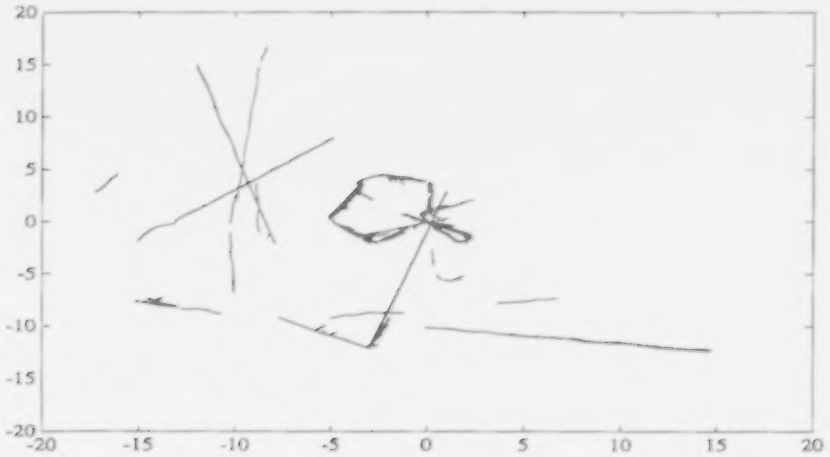

Figure 8.4: **Tracking R1T1 data using Hopfield neural network to implement JPDA**

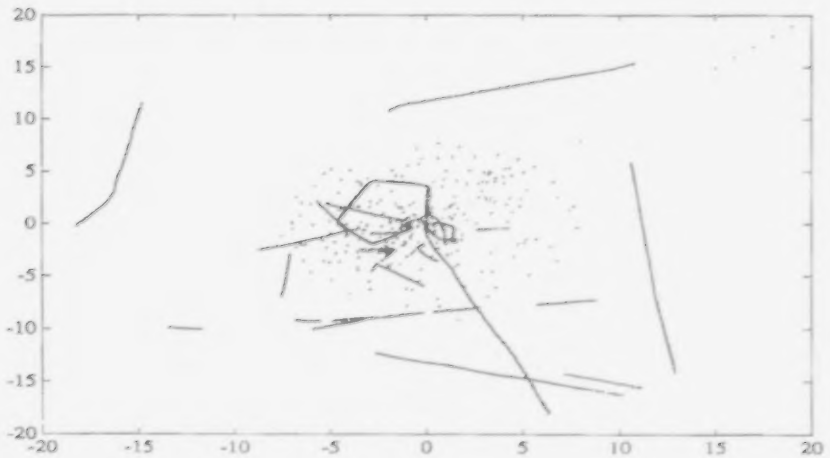

Figure 8.5: **Measured data of R1T2**

P148588.PDF [Page: 73 of 88]

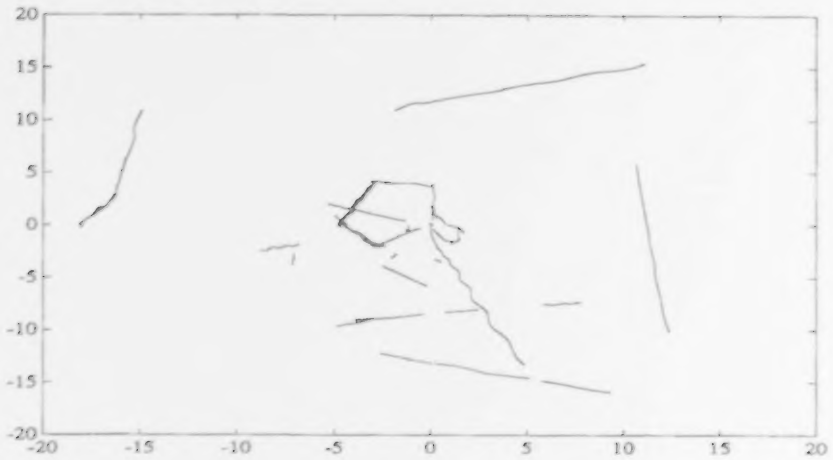

Figure 8.6: **Tracking result of R1T2 using direction PDA**

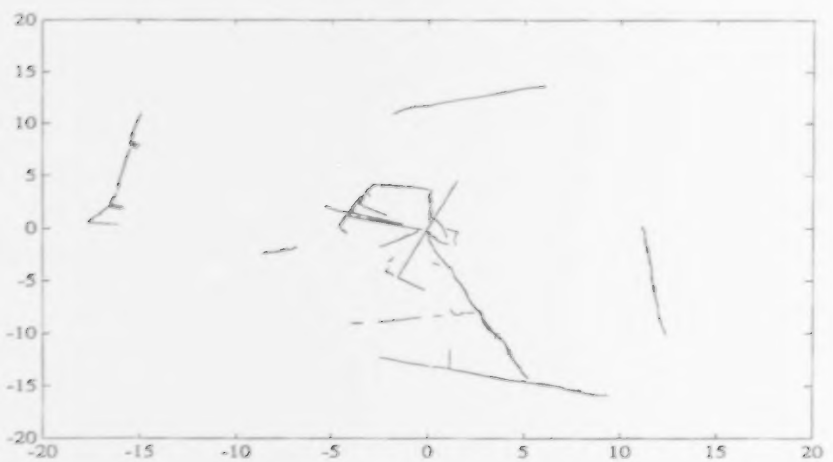

Figure 8.7: **Tracking R1T2 data using Hopfield neural network to implement JPDA**

P148588.PDF [Page: 74 of 88]

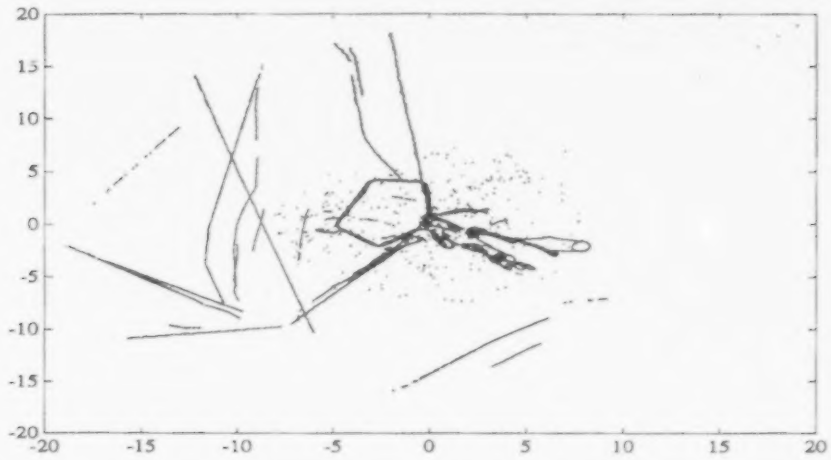

Figure 8.8: **Measured data of R2T1**

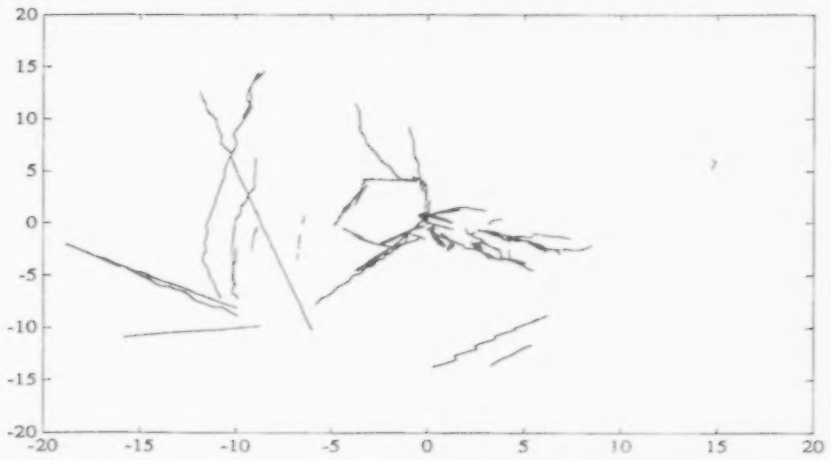

Figure 8.9: **Tracking result of R2T1 using direction PDA**

P148588 PDF [Page: 75 of 88]

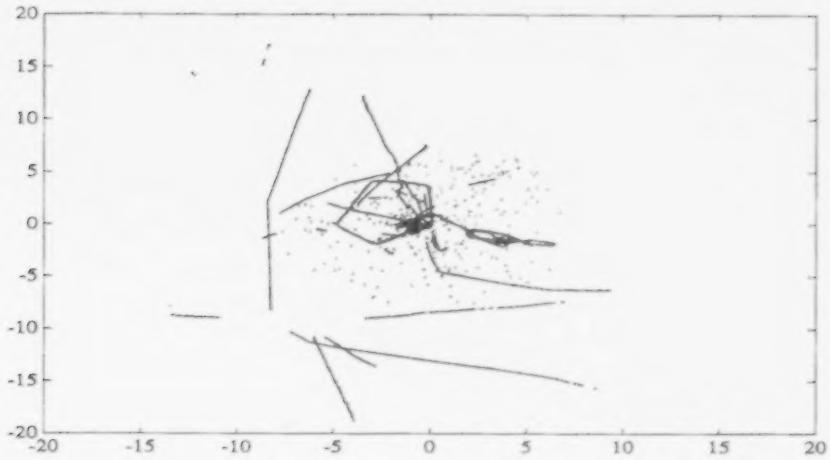

Figure 8.10: **Measured data of R2T2**

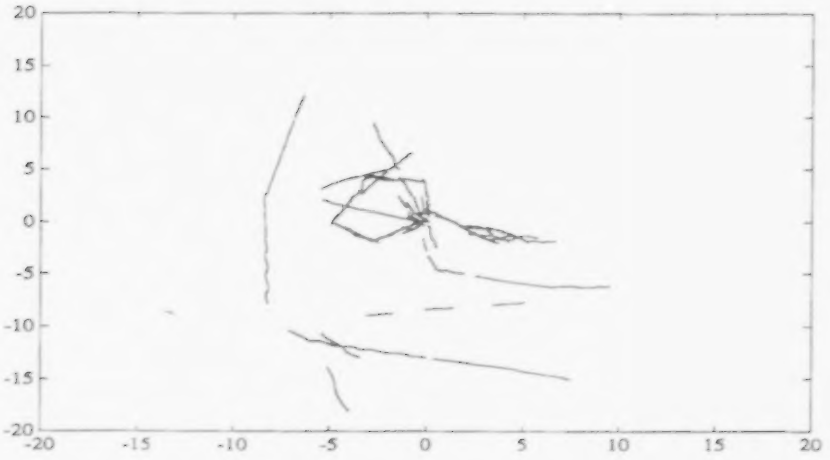

Figure 8.11: **Tracking result of R2T2 using direction PDA**

P148588.PDF [Page: 76 of 88]

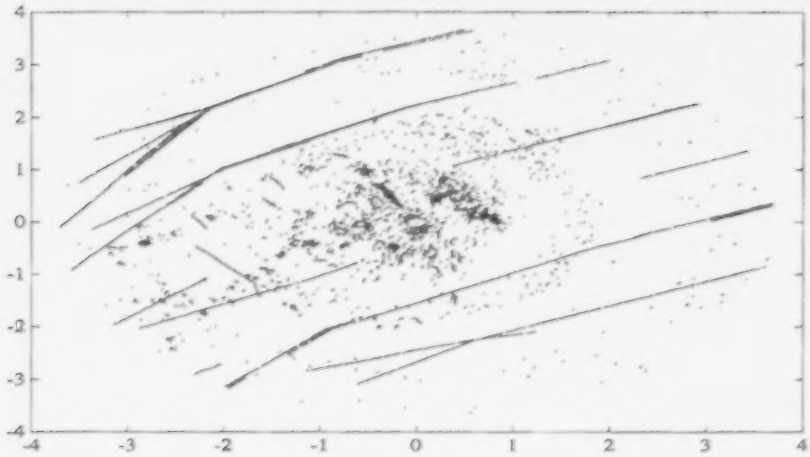

Figure 8.12: **Measured Lab data**

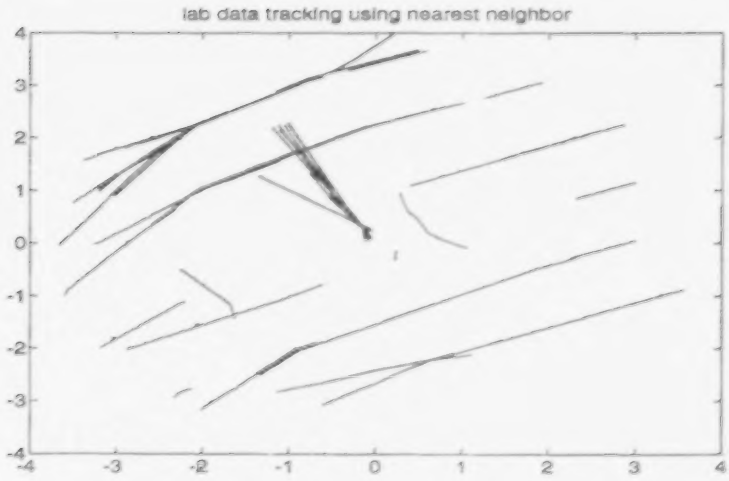

Figure 8.13: **Tracking Result of Lab data using Nearest Neighbor data association**

P148588.PDF [Page: 77 of 88]

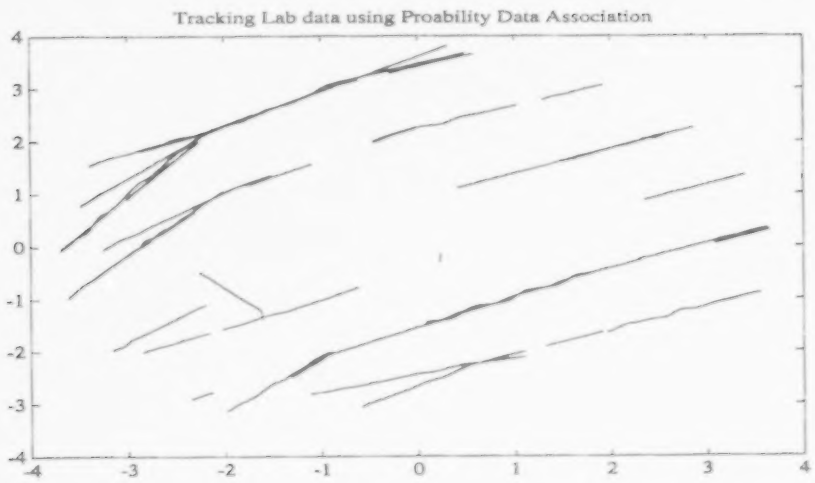

Figure 8.14: **Tracking Result of Lab data using Probability data association**

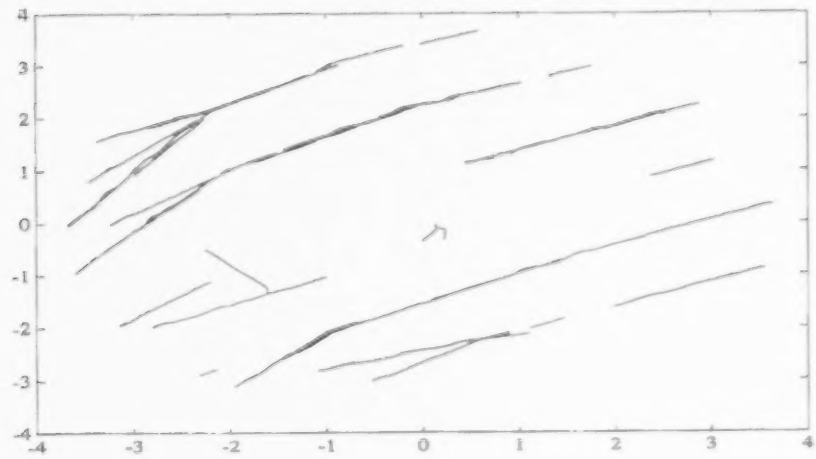

Figure 8.15: **Tracking Result of Lab data using direction probability data association**

P148588.PDF [Page: 78 of 88]

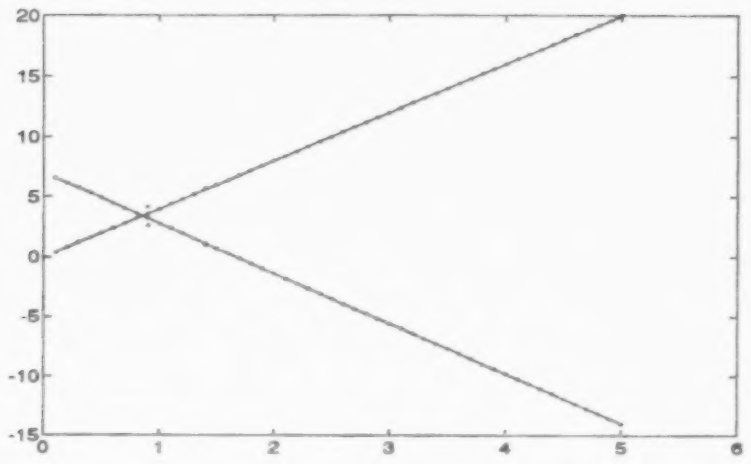

Figure 8.16: **Simulation result of Boltzmann machine implemented JPDA when the number of target is two**

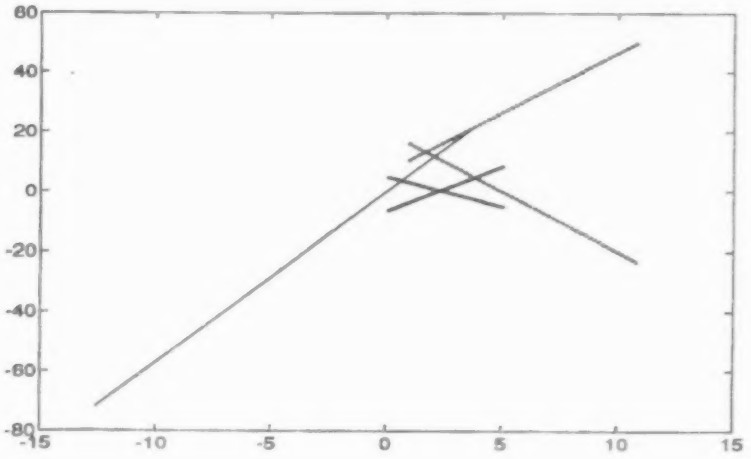

Figure 8.17: **Simulation result of Boltzmann machine implemented JPDA when the number of target is four**

P148588.PDF [Page: 79 of 88]

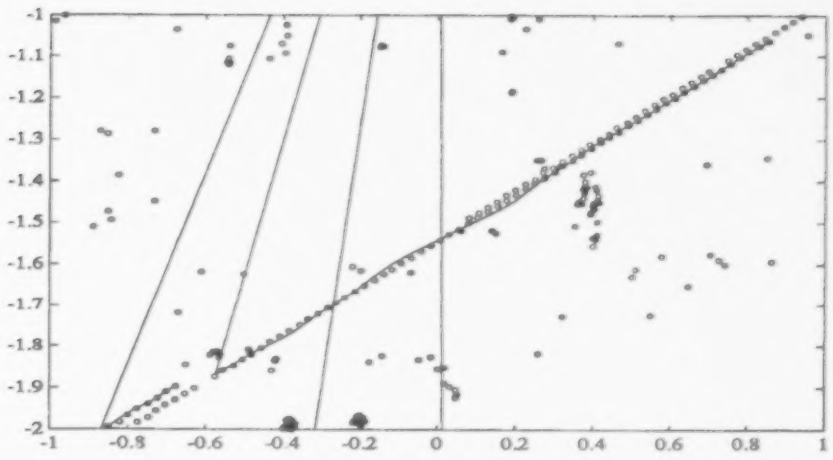

Figure 8.18: **Tracking real data using Boltzmann machine to implement JPDA**

Chapter 9

Conclusions and Recommendations

A software package is developed to implement a technique for multiple-target tracking. The software acquires target range and azimuth information from a radar and is able to identify and track multiple targets in a high clutter environments. The software consists of:

1. Track initiation
2. Gating
3. Prediction and filtering
4. Data association (including Nearest Neighbor, Probability Data Association, Direction Probability Data Association, Hopfield Neural Network implementing Joint Probability Data Association and Boltzmann Machine implementing Joint Probability Data Association).

The processing technique consists of

P148588.PDF [Page: 81 of 88]

1. Tracking Deletion
2. Windowing raw data

The achievements in this report are summarized as following:

1. The new tracking initiation algorithm based on the MHT and Hough Transform has been developed. It was found that this initiation algorithm had much better performance in a clutter environment than standard Hough Transform initiation in terms of false alarm rate. The probability of detection of this new algorithm was close to the probability of detection of Hough Transform initiation.
2. Standard gating, filtering and prediction techniques were used in the MTT.
3. Standard nearest neighbor data association and proability data association has been studied. The standard nestest neighbor has relatively high chance to lose the tracks compared with probability data association in clutter environment. The computational time of PDA does not increase exponentially with the number of targets in the gate.
4. Direction weighting has been incorporated into the probabilities of PDA. It was found that for objects flying in relatively straight lines, direction weighting will give more accurate estimation.
5. Both the Hopfield neural network and the Boltzmann machine implementation for JPDA are investigated.

Base on the findings in this work, it is recommended that

P148588.PDF [Page: 82 of 88]

1. A new initiation algorithm is very effective in the MTT. It is able to identify tracks in a clutter environment with a low false alarm rate. This track initiation technique can replace the standard Hough Transform initiation algorithm.

2. Although the standard gating, prediction and filter techniques used in tracking software produced satisfactory results for both simulated and real data, it is thought that with more realistic noise, such as Glint noise model, estimation would be improved.

3. Data association is the essential part of MTT. For sparse environments, the Nearest Neighbor technique is sufficient. As the target or false return density increases, however, application of Probability Data association technique should be used. As the density further increases, the use of JPDA should be an attractive alternative. Finally, in an extremely dense target environment, such as for tracking convoys of ground targets, the concept of tracking individual targets probability must be abandoned. For a very dense enrironment, targets should be tracked as groups using the methods of group tracking which is basically get the centroid of the group of targets.

4. Both Hopfield neural network and Boltzmann machine implemented Joint Probability Data Association have been incorporated into system. However, the two currently proposed methods are still premature. Further investigation using neural network in MTT is still needed.

P148588.PDF [Page: 83 of 88]

5. Based on discussions with a research scientist at MITRE.[16], it is believed that for maneuvering targets, innovation ideas are needed. Data fusion which combines the tracking with detection would be a good choice for the maneuvering targets.

6. One helpful approach to solve multiple target tracking might be data fusion. Since we have different kinds of sensor in the tracking system, the dimension of observation will be increased. Therefore, with more dimensions of observation, better performance is expected.

P148588.PDF [Page: 84 of 88]

Bibliography

[1] Blackman, S.S. *Multiple-Target Tracking with Radar Applications* , Artech House, 1986

[2] Bar-shalom, Y., and Fortmann, T.E. *Tracking and Data Association*, Academic Press , 1988

[3] Bar-Shalom, Y., and Tse, E. *"Tracking in a cluttered environment with probabilistic data "* Automatica, 11 (Sept. 1975), pp.451–460.

[4] Kolers, Paul A., *Aspects of Motion Perception*, Pergamon Press, 1972.

[5] Fortmann, T. E.,Bar-Shalom, Y., and Scheffe, M. *"Sonar tracking of multiple targets using joint probabilistic data association "* IEEE Journal of Oceanic Engineering, OE–8, 5(July 1983), pp.173–184.

[6] Sengupta, D., and Iltis, R. A. *"Neural Solution to the Multitarget Tracking Data Association Problem "*, IEEE Tran. AES, 1989, pp.96–108.

[7] Hopfield, J. J., and Tank, D.W. *" 'Neural' Computation of Decisions in Optimization Problems "* Biological Cybernetics, 52 (1985), pp.141–152.

P148588.PDF [Page: 85 of 88]

[8] Kim, K., Shafai, B., *" Neural Data Association "* SPIE Vol.1481, 1991, pp.406–417

[9] Casasent, D. P., and Slaski, J., *" Optical track initiator for multitarget tracking"* Applied Optics, Vol. 27, No. 21 November 1988.

[10] Sun, H. M., and Chiang, S. M., *"Tracking Multitarget in cluttered environment"* IEEE Tran. on AES., 1992, pp.546–559.

[11] Iltis, R. A., Ting, Pei–Yih, *"Computing Association Probabilities Using Parallel Boltzmann Machines"* IEEE Tran. on Neural Network, Vol. 4, No. 2, 1993, pp.221–233.

[12] Ting, Pei–Yih, *"An analog diffusion network architecture for solving data association problems in multi–target tracking"*, in Proc. SPIE Conf. Applications of Artificial Neural Networks 3., Orlando, FL, April, 1992

[13] Aarts, E., Korst, J., *"Boltzmann machines for traveling salesman problems,"* European J. Operational Research, vol.39, 1989, pp.79-95.

[14] Aarts, E. and Korst, J., *Simulated Annealing and Boltzmann Machines* New Yourk, Wiley 1989.

[15] Zhou B. and Bose N.K., em "A Comprehensive Analysis of 'Neural Solution to the Multitarget Tracking Data Association Problems", IEEE Tran. AES, vol. 29, No. 1. 1993, pp.260–262.

[16] Private Communication with K. Kim at MITRE Corp.

[17] Wu, W., *"Target tracking with glint noise"*, IEEE Tran. AES, vol. 29, 1993, pp.174–185.

P148588.PDF [Page: 86 of 88]

SECURITY CLASSIFICATION OF FORM
(highest classification of Title, Abstract, Keywords)

DOCUMENT CONTROL DATA

(Security classification of title, body of abstract and indexing annotation must be entered when the overall document is classified)

1. ORIGINATOR (the name and address of the organization preparing the document. Organizations for whom the document was prepared, e.g. Establishment sponsoring a contractor's report, or tasking agency, are entered in section 8.)

McMaster University
1200 Main Street West
Hamilton, Ontario L8N 3Z3

2. SECURITY CLASSIFICATION (overall security classification of the document including special warning terms if applicable)

UNCLASSIFIED

3. TITLE (the complete document title as indicated on the title page. Its classification should be indicated by the appropriate abbreviation (S,C or U) in parentheses after the title.)

A Study of Track Initiation and Data Association for Multiple Target Tracking

4. AUTHORS (Last name, first name, middle initial)

Chen, Ji
Lo, Titus
Litva, John

5. DATE OF PUBLICATION (month and year of publication of document)

August 1993

6a. NO. OF PAGES (total containing information. Include Annexes, Appendices, etc.)

82

6b. NO. OF REFS (total cited i document)

17

7. DESCRIPTIVE NOTES (the category of the document, e.g. technical report, technical note or memorandum. If appropriate, enter the type c report, e.g. interim, progress, summary, annual or final. Give the inclusive dates when a specific reporting period is covered.)

Technical Report

8. SPONSORING ACTIVITY (the name of the department project office or laboratory sponsoring the research and development. Include the address.)

Defence Research Establishment Ottawa
3701 Carling Ave.
Ottawa, Ontario K1A 0K2

9a. PROJECT OR GRANT NO. (if appropriate, the applicable research and development project or grant number under which the document was written. Please specify whether project or grant)

Project 041LO

9b. CONTRACT NO. (if appropriate, the applicable number under which the document was written)

W7714-2-9619/01-ST

10a. ORIGINATOR'S DOCUMENT NUMBER (the official document number by which the document is identified by the originating activity. This number must be unique to this document.)

N/A

10b. OTHER DOCUMENT NOS. (Any other numbers which may be assigned this document either by the originator or by the sponsor)

N/A

11. DOCUMENT AVAILABILITY (any limitations on further dissemination of the document, other than those imposed by security classification

(X) Unlimited distribution
( ) Distribution limited to defence departments and defence contractors; further distribution only as approved
( ) Distribution limited to defence departments and Canadian defence contractors; further distribution only as approved
( ) Distribution limited to government departments and agencies; further distribution only as approved
( ) Distribution limited to defence departments; further distribution only as approved
( ) Other (please specify):

12. DOCUMENT ANNOUNCEMENT (any limitation to the bibliographic announcement of this document. This will normally correspond to the Document Availability (11). However, where further distribution (beyond the audience specified in 11) is possible, a wider announcement audience may be selected.)

P148588.PDF [Page: 87 of 88]

13. ABSTRACT (a brief and factual summary of the document. It may also appear elsewhere in the body of the document itself. It is desirable that the abstract of classified documents be unclassified. Each paragraph of the abstract shall begin with an indication of the security classification of the information in the paragraph (unless the document itself is unclassified) represented as (S), (C), or (U). It is not necessary to include here abstracts in both offical languages unless the text is bilingual).

Multiple target tracking (MTT) is an essential requirement for surveillance system emloying one or more sensor, together with computer subsystems, to interpret an environment that includes both true targets and clutters. With the recent proliferation and the increasing sophistication of surveillance systems, designers of radar and other systems are recognizing the importance of MTT. Therefore, a large amount of literature emerged in recent years. However, in most of the literature, simulated data were used to the MTT algorithms. Thus simplifications, such as that tracks already exist and that the dynamics are known, are assumed. In a real system where the only known information is the measurement returns, the capability of these algorithm becomes questionable.

In this report, a MTT algorithm is developed. Following the discussion of the problem of multiple target tracking, a new track initiation algorithm is proposed and implemented in the system. This new initiation algorithm combines the idea of multiple hypothesis tracking with the standard Hough transform for track initiation. Only a few scans of radar returns are required. Data association is the essential part in the MTT in track maintenance. The performance comparison of three data association algorithms(nearest neighbor, data association, probability data association and direction probability data association) is presented in terms of the percentage of lost tracks in a clutter environment and the percentage of lost tracks in noise environment. Real data test results are also shown. In addition, two kinds of neural network were used to implement the joint probability data association. Both simulated and real data test were used to investigate the performance of the neural networks for the data association.

14. KEYWORDS, DESCRIPTORS or IDENTIFIERS (technically meaningful terms or short phrases that characterize a document and could be helpful in cataloguing the document. They should be selected so that no security classification is required. Identifiers, such as equipment model designation, trade name, military project code name, geographic location may also be included. If possible keywords should be selected from a published thesaurus, e.g. Thesaurus of Engineering and Scientific Terms (TEST) and that thesaurus-identified. If it is not possible to select indexing terms which are Unclassified, the classification of each should be indicated as with the title.)

multiple target tracking, track initiation, Hough transform, data association, nearest neighbor, direction probability, Hopfield neural network, Boltzmann machine